IEEE Access
Multidisciplinary ⋮ Rapid Review ⋮ Open Access Journal

Received 9 September 2023, accepted 25 September 2023, date of publication 6 October 2023, date of current version 17 October 2023.

Digital Object Identifier 10.1109/ACCESS.2023.3322658

RESEARCH ARTICLE

Joint Hybrid Precoding and Combining Design Based Multi-Stage Compressed Sensing Approach for mmWave MIMO Channel Estimation

BAGHDAD HADJI[1], ABDELDJALIL AÏSSA-EL-BEY[2], (Senior Member, IEEE), LAMYA FERGANI[1], AND MUSTAPHA DJEDDOU[3]

[1]LISIC Laboratory, University of Science and Technology Houari Boumediene, Bab Ezzouar, Algiers 16111, Algeria
[2]UMR CNRS 6285 Lab-STICC, IMT Atlantique, 29238 Brest, France
[3]Ecole Nationale Polytechnique, El Harrach, Algiers 16000, Algeria

Corresponding author: Baghdad Hadji (hadjb.ebm@gmail.com)

ABSTRACT Although the design of hybrid precoders and combiners separately from the complete channel state information (CSI) offers satisfactory performance, the resulting spatial multiplexing channel may not always be orthogonal during communication. Also, acquiring CSI to design optimal precoders and combiners poses several challenges, particularly in millimeter wave (mmWave) channel estimation, and getting the sensing matrix is equivalent to designing the precoders and combiners. For this, we propose a new iterative method based on alternating minimization to design the optimal sensing matrix (incoherent projection matrix) with the given dictionary to minimize the mutual coherence values (μ_{mx}, μ_{ave} and μ_{all}) simultaneously according to the equiangular tight frame (ETF) properties for achieving better-compressed sensing (CS) recovery performance. Then, in order to derive the best hybrid precoders and combiners jointly from the optimally designed sensing matrix, we formulate the optimization design problem as the nearest Kronecker product (NKP) problem. The proposed sensing matrix design works better at lowering the mutual coherence values concurrently with the straightforward shrinkage function, according to simulation findings of mutual coherence values evolution versus outer iteration numbers. In comparison to existing codebook-based hybrid precoder/combiner schemes, the proposed joint hybrid precoder and combiner design improves the performance of the simulation results obtained by multi-stage CS-based mmWave channel estimation in terms of channel estimation accuracy and spectral efficiency (SE).

INDEX TERMS Millimeter-wave channel estimation, multi-stage CS approach, hybrid mmWave MIMO transceiver, joint hybrid precoder and combiner design, equiangular tight frame, mutual coherence values, incoherent projection matrix.

I. INTRODUCTION

Due to the bandwidth scarcity in the sub-6 GHz radio spectrum, all cutting-edge signal processing methods in this band have numerous challenges in order to meet the enormous demand for high data rate wireless communication. In order to address the increasing expansion of mobile network data traffic and high-speed communication requirements, a new spectrum band is the primary option. Therefore, due to its potential enormous spectrum resources to achieve multiGigabit-per-second (Gbps) data rates and provide a great opportunity to meet the capacity requirements of future-generation wireless systems and networks, millimeter wave (mmWave) communications are thought to be a promising candidate technology for the new era of wireless communications [1], [2], [3], [4]. Large bandwidth channels are actually the key advantage of switching to mmWave carrier frequencies [5]. However, despite the mmWave spectrum's wide bandwidth, mmWave signals are highly vulnerable to environmental and climate variables, which

The associate editor coordinating the review of this manuscript and approving it for publication was Adao Silva.

result in significant path loss, numerous blockages, and significant penetration losses [6], [7]. Unexpectedly, the increased signal-to-noise ratio (SNR) advantages will boost the capacities of wireless communications. As is common knowledge, using N antennas improves the SNR in the receiver side by $10\log_{10}(N)$ and increases the signal intensity by a factor of $20\log_{10}(N)$ in the transmit side in the desired direction [8]. Therefore, concentrating the highest signal gain within the desired directivity is crucial to overcoming the overall propagation losses when employing a multiple-input multiple-output (MIMO) system [9], [10]. A large number of antenna elements can be deployed at the mmWave transceiver devices in a reasonable physical form factor thanks to the small wavelength of mmWave signals. To apply MIMO in mmWave communications, hybrid architectures have attracted considerable attention as an efficient and promising candidate to strike a better balance among power consumption, hardware complexity, and system performance. Typically, when wireless communication devices are equipped with large antenna arrays, communication protocols are based on signal processing techniques such as precoding and combining. The precoding and combining matrices must be developed from complete knowledge of channel state information (CSI) decomposition for attaining optimal results similar to the ideal performance [11], [12], [13]. This will enable numerous independently controlled beams to be generated with the highest gains. In contrast, due to the substantial training overhead associated with the usage of large antenna arrays at the transceivers and the extremely low received SNR prior to beamforming as a result of the increased noise produced by the huge bandwidth, acquiring the mmWave channel is a challenging process [14]. Therefore, the primary challenge for mmWave MIMO communication systems is hybrid beamformer designs. Due to the use of large antenna arrays for mmWave signals and their limited-scattering propagation, mmWave MIMO channels have sparse structures that easily allow the leveraging of compressed sensing (CS) tools and approaches to develop the mmWave channel estimation algorithm [15]. On the other hand, despite the blessing ability of the CS reconstruction approach to recover the high-dimension channels, beam training is the primordial step in the sparse mmWave channel estimation process as a spatial searching mechanism, where the estimation performance is based on the design quality of beams and their selection strategies [16]. To avoid exhaustive beam training, the authors in [17], [18], [19], and [20] proposed an adaptive CS algorithm with a predesigned multi-resolution hierarchical codebook for developing multi-layer beam selection strategies. For adaptive CS-based channel estimation methods, the hybrid precoding problem is formulated as an Euclidean norm-minimization between the established precoder from the hierarchical codebook at each stage and predefined analog beam set to design the analog and digital precoders. In [15], the analog beam sets generation is complex to realize accurate RF phase shifters due to a large number of quantization bits. To avoid the limitations of the quantized phase shifters, the proposed beamspace MIMO method in [21] can transform the conventional spatial channel into a beamspace channel to capture the sparsity of channel by using the lens antenna array. Unfortunately, this method does not provide uniform performance across a broad range of angles [22]. In [20], an adaptive CS-based mmWave channel estimation algorithm using parallel beams powered by orthogonal sequences are developed to generate narrow multi-resolution beams with low complexity and without power allocation for reducing the complexity of hybrid architecture. Nevertheless, the computational complexity of the designed multi-resolution codebooks increases linearly with the number of dominant channel paths. To avoid excessive channel feedback requirements during the estimation process, CS-based open-loop techniques proposed in [23], [24], and [25] are used to perform the estimation of the mmWave channel explicitly with low computational complexity whatever the number of paths. These techniques apply the CS formulation directly for allowing the use of greedy algorithms with a low mutual coherence as recovery guarantees to improve the channel estimation accuracy. The CS formulation problem in [23] is solved thanks to the orthogonal matching pursuit (OMP) algorithm by employing a redundant dictionary as a sensing matrix on which the design of optimal beam patterns is based on the minimum total coherence (MTC). In [24], a design of a completely deterministic beamformer codebook and pilot symbols are proposed to minimize mutual coherence by using a precoder column ordering algorithm, where the pilot symbol columns are chosen from the discrete Fourier transform (DFT) matrix. In general, the orthogonality of the deterministic pilots is limited by their number. For this reason, the pilot orthogonality in [24] is affected, because the pilot column size is equal to RF chain numbers in hybrid mmWave MIMO systems. Unlike the design of symbol pilots based on the total coherence minimization problem, the authors in [25] decompose the minimization problem into separate transmit and receive coherence minimization problems. In our previous work [26], we proposed a multi-stage CS-based algorithm to estimate the channel of the hybrid mmWave MIMO transceiver by using limited random pilot numbers and detected data symbols as training beams for reducing the effect of the overlapping between training beams throughout the estimation process to maximize spatial diversity. In the all discussed works above, the hybrid precoder and combiner are designed separately to estimate the mmWave channel. Although satisfactory performance is provided by the separate design of the hybrid precoder and combiner, the orthogonality of the resulting spatial multiplexing channel cannot be guaranteed [27]. Therefore, the conventional hybrid precoder and combiner designs may cause significant performance loss in realistic mmWave multiplexing system [28]. In [4] and [28], the joint precoding and combining design are considered by assuming the perfect

CSI which is hard to acquire in mmWave systems as mentioned above. The quality of the equivalent dictionary, which is essential for improving the accuracy of estimation algorithm-based open loop techniques, will be taken into consideration for the first time as we build a new method in this paper to jointly design the hybrid precoder and hybrid combiner so as to acquire the mmWave channel. In order to achieve this, our key contributions are listed below:

- We propose a new iterative method based on alternating minimization to design the optimal sensing matrix (incoherent projection matrix) with the given dictionary for minimizing the mutual coherence values (μ_{mx}, μ_{ave} and μ_{all}) simultaneously. And thus to obtain better CS recovery performance by using the classical shrinkage function in the updating process of the target Gram matrix $\tilde{G}_t$. With the help of the suggested technique, we can indirectly take advantage of the lower mutual coherence indices between the dictionary matrix and the sensing matrix as new recovery guarantees to increase the channel estimate accuracy.
- We suggest a new joint hybrid precoder and combiner design method for enhancing the performance in practical mmWave multiplexing systems by suppressing the interference between different data streams. We formulate the optimization design problem as the nearest Kronecker product (NKP) problem to derive the optimal joint design of hybrid precoders and combiners simultaneously from the optimally designed sensing matrix by taking into account the hybrid architecture constraint.
- We use constrained random pilot numbers and detected data symbols that are forming the training beams throughout the estimation process to take advantage of the jointly developed hybrid precoding and combining with the multi-stage CS approach to explicitly estimate the channel of the hybrid mmWave MIMO transceiver. In order to maximize spatial diversity, the multi-stage CS approach-based open-loop technique lowers the influence of training beam overlapping.

The remainder of the paper is structured as follows. For estimating the mmWave channel, we discuss the system model in Section II and review the sparse formulation based on a multi-stage CS technique. In Section III, we first outline the suggested approach for creating the ideal sensing matrix. Section IV then goes into detail about the joint hybrid precoder and combiner design. Section V is devoted to explain how to estimate the mmWave channel using the multi-stage CS approach-based open-loop strategy and the suggested joint hybrid design. The findings of simulation experiments are discussed in Section VI. Section VII presents the conclusion.

The notations used throughout this paper are: $\mathbf{A}$ denotes a matrix, $\mathbf{a}$ is a vector, a is a scalar, and $\mathcal{A}$ is a set. Whereas A^*, A^T,and A^H represents the conjugate, the transpose, and the conjugate transpose of a matrix $\mathbf{A}$, respectively. $\|A\|_F$ and $|A|$ are Frobenius norm and the determinant of matrix $\mathbf{A}$, respectively, and $\mathrm{Tr}(A)$ is a matrix trace. $\|a\|_p$ is $\mathcal{L}_p$ norms of vector $\mathbf{a}$, and $\mathrm{diag}(a)$ is a diagonal matrix with the entries of $\mathbf{a}$ on its diagonal. I_m indicates the identity matrix of size $m \times m$, and $\mathbf{0}_{m\times n}$ is the $m \times n$ all-zeros matrix. $vec(A)$ denotes the vector operator to vectorize matrix $\mathbf{A}$. $[A]_{:,i}$ denotes i^{th} column of the matrix $\mathbf{A}$. $A \otimes B$ is the Kronecker product of $\mathbf{A}$, and $\mathbf{B}$. $\mathcal{CN}(a, A)$ is a complex Gaussian vector with mean $\mathbf{a}$ and covariance matrix $\mathbf{A}$. $\mathbb{E}[.]$ represents expectation.

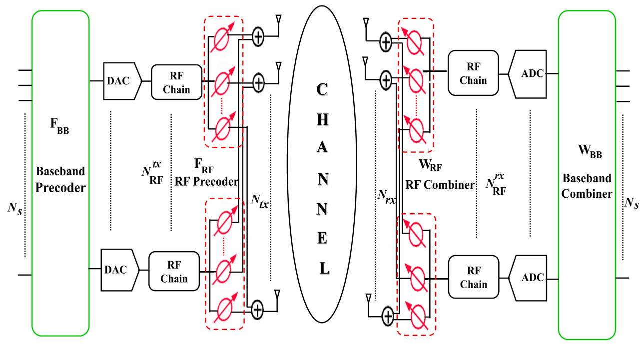

FIGURE 1. Block diagram of hybrid mmWave MIMO architecture with the fully-connected structure.

II. SYSTEM MODEL AND SPARSE FORMULATION

In this section, we present the system model and sparse formulation based on a multi-stage CS approach to estimate the mmWave channel.

A. SYSTEM MODEL

Since the fully connected hybrid MIMO architecture provides full beamforming gain, we consider the hybrid analog/digital MIMO architecture at both the transmitter ($\mathtt{Tx}$) and receiver ($\mathtt{Rx}$) as illustrated in Fig. 1. The $\mathtt{Tx}$ employs $N_{\mathtt{tx}}$ antennas and $N_{RF}^{\mathtt{tx}}$ radio frequency (RF) chains to perform the simultaneous transmission of N_s data streams to the $\mathtt{Rx}$ which is equipped with $N_{\mathtt{rx}}$ antennas and $N_{RF}^{\mathtt{tx}}$ RF chains. For ensuring the effectiveness of multiple stream transmission, N_s is constrained to be bounded at the $\mathtt{Tx}$ and $\mathtt{Rx}$ by $N_s \leq N_{RF}^{\mathtt{tx}} \leq N_{\mathtt{tx}}$ and $N_s \leq N_{RF}^{\mathtt{rx}} \leq N_{\mathtt{rx}}$, respectively. For a practical transceiver architecture, the number of RF chains at the $\mathtt{Rx}$ is usually less than that of the $\mathtt{Tx}$, but without loss of generality, we assume that the number of data streams and the number of RF chains are equal as, $N_s = N_{RF}^{\mathtt{tx}} = N_{RF}^{\mathtt{rx}}$. According to the time-division duplexing protocol (TDD) and the downlink communication scenario, the $\mathtt{Tx}$ precodes the transmitted signal at the time sample n using a hybrid precoder $F_n \in \mathbb{C}^{N_{\mathtt{tx}}\times N_s}$ which can be written as the product of an $N_{RF}^{\mathtt{tx}} \times N_s$ baseband precoder $F_{BB,n}$ and an $N_{\mathtt{tx}} \times N_{RF}^{\mathtt{tx}}$ RF precoder $F_{RF,n}$ where $F_n = F_{RF,n}F_{BB,n}$. Therefore, the discrete-time transmitted signal at the time sample n can be defined as

$$r_n = \sqrt{\gamma}\, F_n x_n = \sqrt{\gamma}\, F_{RF,n} F_{BB,n} x_n \tag{1}$$

where γ represents the average transmit power, and $x_n \in \mathbb{C}^{N_s \times 1}$ is the instantaneous transmitted signal vector. For the hybrid architecture, the total transmit power constraint is enforced by normalizing $F_{BB,n}$ to satisfy $\left\|F_{RF,n}F_{BB,n}\right\|_F^2 = N_s$. Due to the fewer dominant paths and a uniform linear array (ULA) configuration at the transceiver, we adopt the geometric Saleh-Valenzuela model to represent the sparse mmWave channel with L paths as following [23], [24], [25]

$$H = \sqrt{\frac{N_{\mathtt{rx}} N_{\mathtt{tx}}}{L}} \sum_{i=1}^{L} \alpha_i \, a_{\mathtt{rx}}(\theta_i) \, a_{\mathtt{tx}}^H(\phi_i) \tag{2}$$

where α_i is the complex gain of the i^{th} path and it can define the channel type (Rayleigh, Rician or Nakagami), whereas the variables ϕ_i and $\theta_i \in [0, 2\pi]$ are the i^{th} path's azimuth angles of departure and arrival (AoDs/AoAs) of the $\mathtt{Tx}$ and $\mathtt{Rx}$, respectively. The functions $a_{\mathtt{tx}}(\phi_i)$ and $a_{\mathtt{rx}}(\theta_i)$ are the transmit and receive array response vectors corresponding to the i^{th} AoD/AoA, respectively. For a uniform linear array, these functions can be expressed as

$$a_{\mathtt{tx}}(\phi_i) = \frac{1}{\sqrt{N_{\mathtt{tx}}}} \left[1, e^{j\frac{2\pi}{\lambda} d \sin(\phi_i)}, \ldots, e^{j(N_{\mathtt{tx}}-1)\frac{2\pi}{\lambda} d \sin(\phi_i)}\right]^T$$
$$a_{\mathtt{rx}}(\theta_i) = \frac{1}{\sqrt{N_{\mathtt{rx}}}} \left[1, e^{j\frac{2\pi}{\lambda} d \sin(\theta_i)}, \ldots, e^{j(N_{\mathtt{rx}}-1)\frac{2\pi}{\lambda} d \sin(\theta_i)}\right]^T$$

where d denotes the distance between antenna elements, and λ denotes the wavelength of the signal. Moreover, the channel model in (2) can be rewritten in a more compact form as

$$H = A_{\mathtt{rx}} \, H_d \, A_{\mathtt{tx}}^H \tag{3}$$

where $H_d = \operatorname{diag}(\boldsymbol{\alpha})$ is the diagonal path gains matrix, such that $\boldsymbol{\alpha} = \sqrt{\frac{N_{\mathtt{rx}} N_{\mathtt{tx}}}{L}} [\alpha_1, \ldots, \alpha_L]^T$. Whereas, the matrices $A_{\mathtt{tx}} = [a_{\mathtt{tx}}(\phi_1), \ldots, a_{\mathtt{tx}}(\phi_L)]$ and $A_{\mathtt{rx}} = [a_{\mathtt{rx}}(\theta_1), \ldots, a_{\mathtt{rx}}(\theta_L)]$ include the $\mathtt{Tx}$ and $\mathtt{Rx}$ array response vectors.

On the receiving side, the $\mathtt{Rx}$ applies a hybrid combiner $W_n \in \mathbb{C}^{N_{\mathtt{tx}} \times N_s}$ which is composed of an $N_{RF}^{\mathtt{rx}} \times N_s$ baseband combiner $W_{BB,n}$ and an $N_{\mathtt{rx}} \times N_{RF}^{\mathtt{rx}}$ RF combiner $W_{RF,n}$ to process the received signal. Therefore, the received signal vector $y_n \in \mathbb{C}^{N_{\mathtt{tx}} \times 1}$ at the same instant can be expressed as

$$\begin{aligned} y_n &= \sqrt{\gamma} \, W_n^H H F_n x_n + W_n^H \boldsymbol{\eta}_n \\ &= \sqrt{\gamma} \, W_{BB,n}^H W_{RF,n}^H H F_{RF,n} F_{BB,n} x_n + W_{BB,n}^H W_{RF,n}^H \boldsymbol{\eta}_n \end{aligned} \tag{4}$$

where $\boldsymbol{\eta}_n \sim \mathcal{CN}(0, \sigma_\eta^2 I)$ is the additive noise vector. As the analog RF part is implemented by analog phase shifters, $F_{RF,n}$ and $W_{RF,n}$ must be designed by taking into account the constant modulus constraints on their entries.

B. SPARSE FORMULATION BASED ON A MULTI-STAGE CS APPROCH

In this subsection, we revisit the sparse representation of the channel estimation problem proposed in [26] which is based on the multi-stage CS approach. For enabling the sparse formulation of mmWave channel estimation, we exploit the open-loop beam training method, where the $\mathtt{Tx}$ sends M known pilot followed by $N-(M+1)$ unknown data symbols. By vectorizing the right-hand side of the signal model in (4), the received signal vector can be expressed as follows

$$y_n = \sqrt{\gamma} \, (x_n^T F_n^T \otimes W_n^H) \operatorname{vec}(H) + \overline{\boldsymbol{\eta}}_n$$
$$n = 1, \ldots, N \tag{5}$$

where $\overline{\boldsymbol{\eta}}_n = W_n^H \boldsymbol{\eta}_n$ is the noise vector after the hybrid combining. To estimate the sparse mmWave channel by the CS reconstruction, we adopt the concept of the virtual angular domain (VAD) representation [29] to provide a discrete approximation of the physical channel in the quantized angle space. In the VAD representation, the AoDs and AoAs are taken from grids with resolution G, where $\phi_i, \theta_i \in \{0, \frac{2\pi}{G}, \ldots, \frac{2\pi(G-1)}{G}\}$ with $G \gg L$. Then, the physical channel matrix $\mathbf{H}$ in (2) can be rewritten as

$$H = \overline{A}_{\mathtt{rx}} \, \overline{H}_\alpha \, \overline{A}_{\mathtt{tx}}^H \tag{6}$$

where $\overline{H}_\alpha \in \mathbb{C}^{G \times G}$ is a L-sparse channel matrix that stores only L non-zero elements in the positions corresponding to the AoAs and AoDs. $\overline{A}_{\mathtt{rx}} \in \mathbb{C}^{N_{\mathtt{rx}} \times G}$ and $\overline{A}_{\mathtt{tx}} \in \mathbb{C}^{N_{\mathtt{tx}} \times G}$ are angle dictionary matrices which include the steering vectors corresponding to the transmit and receive virtual angle grids with the same resolution at the $\mathtt{Tx}$ and $\mathtt{Rx}$, respectively. By substituting (6) into (5), we exploit the Kronecker product properties to vectorize the channel matrix as $\operatorname{vec}(H) = \boldsymbol{\Psi} h_\alpha$, where $\boldsymbol{\Psi} \in \mathbb{C}^{N_{\mathtt{rx}} N_{\mathtt{tx}} \times G^2}$ is an overcomplete dictionary matrix ($N_{\mathtt{rx}} N_{\mathtt{tx}} < G^2$), such that $\boldsymbol{\Psi} = \overline{\boldsymbol{A}}_{\mathtt{tx}}^* \otimes \overline{\boldsymbol{A}}_{\mathtt{rx}}$. $h_\alpha \in \mathbb{C}^{G^2 \times 1}$ is a vector containing the path gains of the channel matrix $\mathbf{H}$. Hence, the received signal vector in (5) can be expressed as

$$y_n = \sqrt{\gamma} (x_n^T F_n^T \otimes W_n^H) \boldsymbol{\Psi} h_\alpha + \overline{\boldsymbol{\eta}}_n \tag{7}$$

By stacking the N instantaneous received signal vector, we can obtain

$$\begin{aligned} \tilde{y}_G &= \sqrt{\gamma} \left[x_1^T F_1^T \otimes W_1^H, \ldots, x_N^T F_N^T \otimes W_N^H\right]^T \boldsymbol{\Psi} h_\alpha + \tilde{\boldsymbol{\eta}}_G \\ &= \sqrt{\gamma} \left[\boldsymbol{\phi}_1, \ldots, \boldsymbol{\phi}_N\right]^T \boldsymbol{\Psi} h_\alpha + \tilde{\boldsymbol{\eta}}_G \\ &= \sqrt{\gamma} \, \boldsymbol{\Phi}_G \boldsymbol{\Psi} h_\alpha + \tilde{\boldsymbol{\eta}}_G \end{aligned} \tag{8}$$

where $\tilde{y}_G = \left[y_1^T, \ldots, y_N^T\right]^T$ is the collected received signal. $\boldsymbol{\Phi}_G = \left[\boldsymbol{\phi}_1, \ldots, \boldsymbol{\phi}_N\right]^T$ is the global collected sensing matrix (a.k.a projection matrix), where the sensing submatrix at the n^{th} time sample can be defined as $\boldsymbol{\phi}_n = x_n^T F_n^T \otimes W_n^H$, and $\tilde{\boldsymbol{\eta}}_G = \left[\overline{\boldsymbol{\eta}}_1^T, \ldots, \overline{\boldsymbol{\eta}}_N^T\right]^T$ is the collection of the combined noise vector. To apply the multi-stage CS approach, we divide the compressed sensing resulting model in (8) to split the total sensing matrice $\boldsymbol{\Phi}_G$ into two sensing matrices, one corresponds to random pilots and the other corresponds to unknown data symbols as given by

$$\begin{bmatrix} y_1 \\ \vdots \\ y_M \\ y_{M+1} \\ \vdots \\ y_N \end{bmatrix} = \sqrt{\gamma} \begin{bmatrix} \boldsymbol{\Phi}_P \\ \\ \boldsymbol{\Phi}_D \end{bmatrix} \boldsymbol{\Psi} h_\alpha + \begin{bmatrix} \overline{\boldsymbol{\eta}}_1 \\ \vdots \\ \overline{\boldsymbol{\eta}}_M \\ \overline{\boldsymbol{\eta}}_{M+1} \\ \vdots \\ \overline{\boldsymbol{\eta}}_N \end{bmatrix} \tag{9}$$

In the end, we have two separate stages, the M random pilots are used at the first stage to estimate the channel where its received training signal model can be expressed as

$$\tilde{y}_P = \boldsymbol{\Phi}_P \boldsymbol{\Psi} h_\alpha + \tilde{\boldsymbol{\eta}}_P \tag{10}$$

For the second stage, we can exploit the estimated channel from the first stage to detect the unknown data symbols, then the received signal model of the second stage is written as follows

$$\tilde{y}_D = \mathbf{\Phi}_D \mathbf{\Psi} h_\alpha + \tilde{\boldsymbol{\eta}}_D \tag{11}$$

III. SENSING MATRIX DESIGN FOR CS-BASED CHANNEL ESTIMATION

In CS reconstruction, using the mutual coherence minimization directly as a sparse recovery guarantee metric to derive the optimization problem can be misleading [30]. Hence, finding the optimal beamformers design via mutual coherence minimization of the sensing matrix as proposed in [23], [24], and [25] does not always guarantee the CS-based mmWave channel estimation performance. Thus, for recovering the sparse signal with higher accuracy in CS, there must be a smaller mutual coherence between the sensing matrix and the dictionary matrix. As result, CS theory requires that $\mathbf{\Phi}$, the sensing matrix, and $\mathbf{\Psi}$, the dictionary matrix, be as incoherent as possible [31]. In other words, the correlation between any distinct pair of columns in the equivalent dictionary $\mathbf{D}$ ($D = \mathbf{\Phi\Psi}$) should be very small, and that means having a nearly orthogonal dictionary $\mathbf{D}$ [32]. In the CS-based mmWave channel estimation model, designing the sensing matrix is equivalent to designing the precoders and combiners indirectly. For this purpose, we adopt in this work the incoherent projection method to provide an incoherent equivalent dictionary and find the optimal design of the sensing matrix with the given dictionary to improve the estimation accuracy. In the literature, the design of the optimal sensing matrix is achieved by designing an equiangular tight frame (ETF) for the corresponding Gram matrix and updating the frame to reduce the mutual coherence [30]. We should review the definition of mutual coherence indexes and the concept of frames used to design the sensing matrix [31]. Without loss of generality, we take the CS model at first stage as an example to present the proposed method for designing the sensing matrix $\mathbf{\Phi}_P$.

Definition 1: The maximum mutual coherence of a matrix $D_P \in \mathbb{C}^{MN_{RF}^{tx} \times G^2}$, is defined as the largest absolute and normalized inner product between different columns in D_P that can be expressed as

$$\mu_{mx}(D_P) = \max_{i \neq j, 1 \leq i, i \leq G^2} \left\{ \frac{\left| d_{P_i}^T d_{P_j} \right|}{\left\| d_{P_i} \right\|_2^2 \cdot \left\| d_{P_j} \right\|_2^2} \right\} \tag{12}$$

with $\mu_{welch} \leq \mu_{mx}(D_P) \leq 1$, where $\mu_{welch} \triangleq \sqrt{\frac{G^2 - MN_{RF}^{tx}}{MN_{RF}^{tx}(G^2-1)}}$ is the Welch bound or ranking bound. As $D_P = \mathbf{\Phi}_P \mathbf{\Psi}$, the desired $\mathbf{\Phi}_P$ must have a small $\mu_{mx}(\mathbf{\Phi}_P \mathbf{\Psi})$ with respect to $\mathbf{\Psi}$ for obtaining better recovery performance. In the CS framework, the optimal design of $\mathbf{\Phi}_P$ is gained by minimizing the μ_{mx} of the corresponding Gram matrix $\tilde{G}_P = \tilde{D}_P^H \tilde{D}_P$, where $\tilde{D}_P$ is column-normalized version of D_P. In addition, other mutual coherence values of $\tilde{G}_P$ can be used as measure metrics for evaluating the sensing matrix quality. These metrics are the maximum, averaged, and global mutual coherence values (μ_{mx}, μ_{ave} and μ_{all}) of the off-diagonal elements of $\tilde{G}_P$, and they can be expressed respectively as [30], [31], [32], [33], and [34]

$$\mu_{mx} = \max_{i \neq j} \left| \tilde{g}_{P_{ij}} \right| \tag{13}$$

$$\mu_{ave} = \frac{\sum_{i \neq j} \left(\left| \tilde{g}_{P_{ij}} \geq t \right| \right) \left| \tilde{g}_{P_{ij}} \right|}{\sum_{i \neq j} \tilde{g}_{P_{ij}} \geq t} \tag{14}$$

$$\mu_{all} = \sum_{i \neq j} \tilde{g}_{P_{ij}}^2 \tag{15}$$

where $\tilde{g}_{P_{ij}} = \tilde{\boldsymbol{g}}_{P_i}^T \tilde{\boldsymbol{g}}_{P_j}$ is the entry at the position of row i and column j in $\tilde{G}_P$. The value t is the threshold proposed by Elad [34] to minimize the mutual coherence where $\mu_{ave} \geq t$. To obtain the best sparse recovery, the incoherence of the equivalent dictionary must achieve the Welch bound as a minimal correlation between any pair of columns. Thanks to ETF properties, the different mutual coherence values can reach the Welch bound [35]. As a result, optimizing a dictionary to approximate ETF is an effective method to design the sensing matrix with minimizing the mutual coherence values [30]. As frames play a crucial role to get the optimal sensing matrix, we briefly revisit the concept of a frame and its important properties in the general framework.

Definition 2: The matrix $D = [d_1, \ldots, d_n] \in \mathbb{C}^{m \times n}$ is called a frame with $m \ll n$, if there exist two constants $0 < \alpha \leq \beta \leq +\infty$ such that

$$\alpha \left\| v \right\|_2 \leq \left\| D^T v \right\|_2 \leq \beta \left\| v \right\|_2, \forall v \in \mathbb{C}^m \tag{16}$$

where α and β are the lower and the upper bound of frames respectively [36]. If $\alpha = \beta$ in (16), the frame $\mathbf{D}$ is called α-tight frame, and when $\alpha = \beta = 1$, is called a Parseval frame.

Definition 3 (see [37]): Let $D \in \mathbb{C}^{m \times n}$ with $m \ll n$ whose columns are $d_1, d_2, \ldots, d_n$. The overcomplete dictionary $\mathbf{D}$ is called ETF, if the following conditions are satisfied

- Each column has a unit norm: $\|d_i\|_2$ for $i = 1, \ldots, n$.
- The columns are equiangular. For some nonnegative δ, we get $\left| d_i^T d_j \right| = \delta$ when $i \neq j,\ i, j = 1, \ldots, n$.
- The columns form a tight frame. That is, $DD^H = \left(\frac{n}{m}\right) I_m$, where I_m is identity matrix of size $m \times m$.

According to the definition (2) and (3), frames are an overcomplete version of a basis set and tight frames are an overcomplete version of an orthogonal basis set [30], [32]. Whereas, the ETF generalizes the geometric properties of an orthonormal basis [37]. To design the sensing matrix based on the ETF properties, many algorithms are proposed to solve the minimizing problem of the Frobenius norm of the difference between the Gram matrix and the target Gram matrix [32], [34], [38]. For the first stage, the collected sensing matrix design problem with respect to $\mathbf{\Psi}$ can be formulated as

$$\arg\min_{\Phi_P, \tilde{G}_{tp}} \left\| \tilde{G}_{tp} - \Psi^H \Phi_P^H \Phi_P \Psi \right\|_F^2 \tag{17}$$

where the target gram matrix $\tilde{G}_{tp}$ is chosen from a convex set $\mathcal{H}_{\mu_{welch}}$ which contains the ideal ETF [39]

$$\mathcal{H}_{\mu_{welch}} = \Big\{ \tilde{G}_{tp} \in \mathbb{C}^{G^2 \times G^2} : \tilde{G}_{tp} = \tilde{G}_{tp}^H, \operatorname{diag}(\tilde{G}_{tp}), \max_{i \neq j} \left| \tilde{G}_{tp}(i,j) \right| \leq \mu_{welch} \Big\} \tag{18}$$

From the cost function in (17), the main minimization problem challenges are finding the ideal $\tilde{G}_{tp}$ which is close as possible to an ETF and the optimal design of Φ_P simultaneously. In [34], an iterative approach is developed to reduce the t-averaged mutual coherence (14) as recovery guarantee metric. However, this design approach cannot reach the optimal solution for μ_{mx} and μ_{ave}, respectively, which ruins the worst-case guarantees of the reconstruction algorithms. Authors in [32] propose a gradient-based alternating minimization approach to update the projection matrix with a target Gram matrix. To decrease the above three mutual coherence values simultaneously, new thresholding of the shrinkage function is developed in [38] for reducing the off-diagonal elements of the target Gram matrix. The main drawback of this shrinkage approach is that there is no analytical solution to find a suitable threshold for any CS applications. Our main goal is to design the sensing matrix and solve the problem in (17) with classical target gram matrix design defined in (18) for minimizing the mutual coherence values simultaneously. Algorithm 1 summarizes all steps for designing the optimal sensing matrix. Starting with the first stage, Φ_P is constructed by random pilots and hybrid training precoders/combiners which are generated randomly using six quantization bits to design RF phase shifters according to the multi-stage CS approach [26]. Moreover, we introduce Ψ as a given sparsifying dictionary to get the equivalent dictionary $D_P = \Phi_P \Psi$. Afterward, we normalize the columns in D_P during each iteration to provide a column-normalized version of the equivalent dictionary $\tilde{D}_P$ that is used to compute the gram matrix as $\tilde{G}_P = \tilde{D}_P^H \tilde{D}_P$.

According to ETF properties, we update $\tilde{G}_{tp}$ to be close to the corresponding ETF designed by projecting the Gram matrix elements $g_{tP_{ij}}$ on $\mathcal{H}_{\mu_{welch}}$ to have unit diagonal elements and reducing the off-diagonals by using the Welch bound as

$$\forall\, i,j \;\; i \neq j : \tilde{G}_{tp}(i,j) = \begin{cases} \tilde{g}_{tP_{ij}} & \left| g_{tP_{ij}} \right| < \mu_{welch} \\ \operatorname{sign}(\tilde{g}_{tP_{ij}}) & \text{otherwise} \end{cases} \tag{19}$$

In this paper, the optimal sensing matrix is obtained by the following theorem for minimizing mutual coherence values simultaneously

Theorem 1: Let $\Psi = U_\Psi \left[\Sigma_\Psi \;\; \mathbf{0}\right] V_\Psi^H$ be an SVD of Ψ where $U_\Psi \in \mathbb{C}^{m \times m}$ and $V_\Psi \in \mathbb{C}^{n \times n}$ are unitary matrices,

Algorithm 1 Sensing Matrix Designing Algorithm

Input: sparsifying basis Ψ which has an SVD form $\Psi = U_\Psi \left[\Sigma_\Psi \;\; \mathbf{0}\right] V_\Psi{}^H$,
μ_{welch}, number of iterations *Iter*
Output: Sensing matrix $\hat{\phi}_P$
Initialization: Create Φ_P with randomly generation of F/W and random pilots
for k to *Iter* **do**
1) $\Phi_{P_{(k)}} \leftarrow \Phi_P$
2) Compute the equivalent matrix $D_P = \Phi_{P_k} \Psi$
3) Compute the Gram matrix $\tilde{G}_P = \tilde{D}_P^H \tilde{D}_P$ ($\tilde{D}_P$ is normalization version of D_P)
4) Update $\tilde{G}_P$ to obtain $\tilde{G}_{tp}$ using (19)
5) Compute the positive semidefinite matrix $\Theta = V_\Psi^H \tilde{G}_{tp} V_\Psi$
6) Apply eigenvalue decomposition to obtain $\Theta = X_\Theta A_\Theta X_\Theta{}^H$
• Find $\Lambda_\Theta \in \mathbb{C}^{m \times m}$ including m maximum eigenvalues of A_Θ
• Find $P \in \mathbb{C}^{n \times m}$ containing the first columns of X_Θ
7) Update $\Phi_{P_{(k+1)}}$ using (20)
end for

if $\operatorname{Rank}(\Psi) = m < n$ the matrix Σ_Ψ contains m singular values with $\sigma_1 \geq \sigma_2 \ldots \geq \sigma_m$. Suppose that $\tilde{G}_{tp} \in \mathcal{H}_{\mu_{welch}}$, if $\Theta = V_\Psi^H \tilde{G}_{tp} V_\Psi$ is positive semidefinite matrix, then $\Theta = X_\Theta A_\Theta X_\Theta{}^H$ is the eigendecomposition of Θ. The optimal $\Phi_{P_{opt}}$ can be find by the following solution to solve the problem in (17)

$$\Phi_{P_{opt}} = \Lambda_\Theta{}^{\frac{1}{2}} P^H \left[\Sigma_\Psi^{-1} \;\; \mathbf{0}\right]^H U_\Psi{}^H \tag{20}$$

where $\Lambda_\Theta \in \mathbb{C}^{m \times m}$ is diagonal matrix that contain m maximum eigenvalues of Θ, whereas $P \in \mathbb{C}^{n \times m}$ denotes the first m columns of X_Θ corresponding to the top m eigenvalues.

The proof of this theorem is detailed in the Appendix A.

IV. JOINT HYBRID PRECODER AND COMBINER DESIGN

In this section, we present the proposed joint hybrid precoder and combiner design method to improve the multiplexing performance in practical mmWave systems by suppressing the interference between different training beams. After the design of the collected sensing matrix at first stage by using the algorithm 1, we can jointly design each precoder and combiner at each n^{th} time sample. Since the collected sensing matrix at the first stage is the concatenation of n^{th} sensing submatrix, the optimal sensing matrix can be written as $\hat{\phi}_P = \left[\hat{\phi}_1, \ldots, \hat{\phi}_M\right]^T$ with M is the random pilot numbers where each optimal sensing submatrix at the m^{th} sample can be rewritten as $\hat{\phi}_m = \bar{s}_m^T \otimes W_m$, the precoder pilot $\bar{s}_m$ is defined as $\bar{s}_m = F_m x_m$. Therefore, the joint hybrid precoder/combiner design problem can be expressed as

$$\{\bar{s}_m^{opt}, W_m^{opt}\} = \arg\min_{\bar{s}_m^{opt}, W_m^{opt}} \left\| \hat{\boldsymbol{\phi}}_m - \bar{s}_m^T \otimes W_m^H \right\|_F \quad \text{s.t.} \quad \|\bar{s}_m \otimes W_m\|_F^2 \leq N_{RF}^{\mathtt{rx}} \tag{21}$$

This optimization problem is similar to the NKP problem. In [40], the authors propose a general technique to establish a key result that converts this minimization problem to a $rank-1$ approximation problem as the following theorem

Theorem 2 (see [40]): Assume that $A \in \mathbb{R}^{m\times n}$ with $m = m_1m_2$ and $n = n_1n_2$. If $B \in \mathbb{R}^{m_1\times n_1}$ and $C \in \mathbb{R}^{m_2\times n_2}$, then

$$\|A - B\otimes C\|_F = \left\| \mathcal{R}(A) - vec(B)vec(C)^T \right\|_F \tag{22}$$

where $\mathcal{R}(A)$ define the rearrangement of $\mathbf{A}$ after applying the *vec* operator on each submatrix A_{ij} in $\mathbf{A}$ and stacking its columns as this example, for the 2-by-2 blocks of $\mathbf{A}$, $\mathcal{R}(A)$ can be written as

$$A = \begin{bmatrix} A_{11} & A_{12} \\ A_{21} & A_{22} \end{bmatrix} \Rightarrow \mathcal{R}(A) = \begin{bmatrix} vec(A_{11})^T \\ vec(A_{21})^T \\ vec(A_{12})^T \\ vec(A_{22})^T \end{bmatrix} \tag{23}$$

The approximation of a given matrix by a $rank-1$ matrix has a well-known solution in terms of the singular value decomposition (SVD) [40]. Since the SVD decomposition is a general form of the eigendecomposition for any matrix. The solution to the optimization problem in (21) can be found by computing the largest singular value and associated singular vectors of a permuted version of $\hat{\boldsymbol{\phi}}_m$ as $\mathcal{R}(\hat{\boldsymbol{\phi}}_m)$. Therefore, the joint hybrid precoding and combining will be designed by the corollary below.

Corollary 1 (see [40]): Assume that $A \in \mathbb{R}^{m\times n}$ with $m = m_1m_2$ and $n = n_1n_2$. If $\tilde{A} = \mathcal{R}(A)$ has singular value decomposition

$U^T\tilde{\boldsymbol{A}}V = \boldsymbol{\Sigma} = \mathrm{diag}(\sigma_i)$

where σ_1 is the largest singular value, and $U(:,1)$ and $V(:,1)$ are the corresponding singular vectors, then the matrices $B \in \mathbb{C}^{m_1\times n_1}$ and $C \in \mathbb{C}^{m_2\times n_2}$ defined by $vec(B)^{opt} = \sqrt{\sigma}_1\boldsymbol{U}(:,1)$ and $vec(C)^{opt} = \sqrt{\sigma}_1\boldsymbol{V}(:,1)$ minimize $\|A - B\otimes C\|_F$.

To deal with the hybrid architecture, we add the total transceiver power constraint to ensure the efficiency of the communication. The total transceiver power can be defined in our case as follows

Lemma 3: Let $z \in \mathbb{C}^m$ be a vector such that $\|z\|_2^2 = 1$, and $\boldsymbol{\Gamma} \in \mathbb{C}^{m\times n}$ be an arbitrary matrix, then

$$\|z\otimes\boldsymbol{\Gamma}\|_F^2 \leq \|\boldsymbol{\Gamma}\|_F^2 \tag{24}$$

The proof of this lemma is detailed in the Appendix B. Based on this lemma, we define the added power constraint in (21) to bound the total power of hybrid communication system with limited number of RF chains as $\left\|\bar{s}_m^{opt} \otimes W_m^{opt}\right\|_F^2 \leq N_{RF}^{\mathtt{tx}}$. From the previous discussion, it is clear that the optimal sensing matrix design plays an important role to design hybrid precoders/combiners and offers the satisfactory performance improvement. After the design of the optimal sensing matrix by using the algorithm 1. The proposed approach to design the jointly hybrid precoding and combining is summarized in Algorithm 2 that starts by the initialization process to divide $\boldsymbol{\Phi}_P$ into submatrix sets Ξ where each submatrix has the size of $N_{RF}^{\mathtt{tx}} \times N_{\mathtt{tx}}N_{\mathtt{rx}}$, which means that each submatrix represents an optimal sensing submatrix $\hat{\boldsymbol{\phi}}_m$ that is corresponding to the m^{th} time sample. In step (1), each optimal sensing submatrix $\hat{\boldsymbol{\phi}}_T$ is extracted from submatrix sets Ξ to construct the rearrangement of $\hat{\boldsymbol{\phi}}_T$ using equation (23) for the purpose of formulating the $rank-1$ approximation problem as shown in theorem (2). Then, SVD decomposition of resultant matrix $\mathcal{R}(\hat{\boldsymbol{\phi}}_T)$ is computed in step (3). As $\hat{\boldsymbol{\phi}}_T$ is separable, such that $\hat{\boldsymbol{\phi}}_T = \bar{s}_m^T \otimes W_m^H$, the largest singular value and corresponding singular vectors are found by the corollary (1) to minimize the objective in (21). After finding $\bar{s}_T^{opt}$ and W_T^{opt}, the transceiver power constraint is enforced by normalizing the transpose of $\bar{s}_T^{opt}$ and conjugate of W_T^{opt}. Finally, each designed precoder and combiner are appended to $\bar{S}^{opt}$ and W^{opt} matrices respectively at each iteration. The process is repeated for all M random pilot numbers until all precoder and combiner vectors of the first stage have been designed.

Algorithm 2 Joint Hybrid Precoding and Combining Design Algorithm

Input: $\hat{\boldsymbol{\phi}}_P$, $N_{\mathtt{tx}}$, $N_{\mathtt{rx}}$, $N_{RF}^{\mathtt{tx}}$, $N_{RF}^{\mathtt{rx}}$, M
Output: $\bar{S}^{opt}$, W^{opt}
Initialization:
- divide $\hat{\boldsymbol{\phi}}_P$ into submatrix sets Ξ each one has the size of $N_{RF}^{\mathtt{tx}} \times N_{\mathtt{rx}}N_{\mathtt{rx}}$
- $\bar{S}^{opt}$ an empty matrix to concatenate $\bar{s}_m^{opt}$
- W^{opt} an empty matrix to concatenate W_m^{opt}

for T to M **do**
1) $\hat{\boldsymbol{\phi}}_T = \Xi\{T\}$ ▷ extract each submatrix
2) construct $\mathcal{R}(\hat{\boldsymbol{\phi}}_T)$ using equation in (23)
3) Computing SVD decomposition of $\mathcal{R}(\hat{\boldsymbol{\phi}}_T)$
4) Find $\bar{s}_T^{opt}$ and W_T^{opt} using corollary (1)
5) $\bar{S}^{opt}\{T\} = \frac{(\bar{s}_T^{opt})^T}{\left\|(\bar{s}_T^{opt})^T\right\|_2}$
6) $W^{opt}\{T\} = \sqrt{N_{RF}^{\mathtt{rx}}}\frac{(W_T^{opt})^H}{\left\|(W_T^{opt})^H\right\|_F}$

end for

For computational complexity evaluation, we exploit the required number of floating point operations (FLOPs) as a evaluation metric with $\mathcal{O}$ notation and omit terms of the low exponent. The complexity of algorithm 2 is dominated by the truncated SVD decomposition in each iteration, where its computational complexity is located at step 3 and it is about $\mathcal{O}(2N_{RF}^{\mathtt{tx}}N_{\mathtt{tx}}N_{\mathtt{rx}})$. Thus, the complexity of algorithm 2 is approximately $\mathcal{O}(2N_{RF}^{\mathtt{tx}}N_{\mathtt{tx}}N_{\mathtt{rx}}M)$ to accomplish the joint design process where the computational load is function of antenna numbers at the transceiver, RF chain numbers at the receiver, and the random pilot numbers.

As mentioned above, the second stage is dedicated to detect unknown data symbols by employing the estimated channel from the first stage. As in [26], we adopt in this work the QPSK modulation scheme to transmit unknown data. From the system model in (11), each sensing submatrix $\boldsymbol{\phi_n}$ of the collected sensing matrix $\boldsymbol{\Phi}_D$ can be expressed as $\boldsymbol{\phi_n} = \left({x_{d,n}}^T {F_{d,n}}^T \otimes {W_{d,n}}^H\right)$, where $F_{d,n}$ and $W_{d,n}$ denote the precoder and combiner that are used to send and measure the unknown data $x_{d,n}$ at the n^{th} time sample with $M+1 \leq n \leq N$. To design the hybrid precoder and combiner jointly, we cancel the effect of unknown data symbols from $\boldsymbol{\Phi}_D$ by averaging the Gram matrix as

$$\begin{aligned}
\mathbb{E}\left[\tilde{G}_D\right] &= \mathbb{E}\left[\tilde{D}_D^H \tilde{D}_D\right] \\
&= \mathbb{E}\left[\boldsymbol{\Psi}^H \boldsymbol{\Phi}_D^H \boldsymbol{\Phi}_D \boldsymbol{\Psi}\right] \\
&= \mathbb{E}\left[\boldsymbol{\Psi}^H \sum_{n=M+1}^{N} {\boldsymbol{\phi_n}}^H \boldsymbol{\phi_n} \boldsymbol{\Psi}\right] \\
&= \mathbb{E}\Bigg[\boldsymbol{\Psi}^H \sum_{n=M+1}^{N} \left({x_{d,n}}^T {F_{d,n}}^T \otimes {W_{d,n}}^H\right)^H \\
&\quad \left({x_{d,n}}^T {F_{d,n}}^T \otimes {W_{d,n}}^H\right) \boldsymbol{\Psi}\Bigg] \\
&= \mathbb{E}\Bigg[\boldsymbol{\Psi} \sum_{n=M+1}^{N} \Big({F_{d,n}}^* {x_{d,n}}^* {x_{d,n}}^T {F_{d,n}}^T \otimes \\
&\quad W_{d,n} {W_{d,n}}^H\Big) \boldsymbol{\Psi}\Bigg] \\
&= \boldsymbol{\Psi}^H \sum_{n=M+1}^{N} \Big({F_{d,n}}^* \underbrace{\mathbb{E}\left[{x_{d,n}}^* {x_{d,n}}^T\right]}_{E_s} \\
&\quad {F_{d,n}}^T \otimes W_{d,n} {W_{d,n}}^H\Big) \boldsymbol{\Psi} \\
&= \left(N - (M+1)\right) E_s \boldsymbol{\Psi}^H \\
&\quad \left({F_D}^* {F_D}^T \otimes W_D {W_D}^H\right) \boldsymbol{\Psi} \\
&= \left(N - (M+1)\right) E_s \boldsymbol{\Psi}^H \left({F_D}^T \otimes {W_D}^H\right)^H \\
&\quad \left({F_D}^T \otimes {W_D}^H\right) \boldsymbol{\Psi}
\end{aligned}$$

$$\mathbb{E}\left[\tilde{G}_D\right] = k \boldsymbol{\Psi}^H \tilde{\boldsymbol{\Phi}}_D^H \tilde{\boldsymbol{\Phi}}_D \boldsymbol{\Psi} \tag{25}$$

where $\tilde{D}_D$ is normalized version of the equivalent dictionary D_D, such that $D_D = \boldsymbol{\Phi}_D \boldsymbol{\Psi}$, and $\boldsymbol{\Psi}$ is the same sparsifying dictionary used at the first stage. E_s represents the energy per symbol and F_D is the precoding matrix given by the concatenation of all m^{th} precoder. Whereas W_D is combining matrix which is containing all combiners at second stage. Before the joint design of hybrid precoding and combining, we must design the collected sensing matrix $\tilde{\boldsymbol{\Phi}}_D$ as applied in the first stage by using the following objective function

$$\begin{cases}
\underset{\tilde{G}_{t_D}}{\arg\min} \left\| \tilde{G}_{t_D} - \mathbb{E}\left[\tilde{G}_D\right] \right\|_F^2 \\
\underset{\tilde{G}_{t_D}, \boldsymbol{\Phi}_D}{\arg\min} \left\| \tilde{G}_{t_D} - \mathbb{E}\left[\boldsymbol{\Psi}^H \boldsymbol{\Phi}_D^H \boldsymbol{\Phi}_D \boldsymbol{\Psi}\right] \right\|_F^2 \\
\underset{\tilde{G}_{t_D}, \tilde{\boldsymbol{\Phi}}_D}{\arg\min} \left\| \tilde{G}_{t_D} - k \boldsymbol{\Psi}^H \tilde{\boldsymbol{\Phi}}_D^H \tilde{\boldsymbol{\Phi}}_D \boldsymbol{\Psi} \right\|_F^2
\end{cases} \tag{26}$$

As $k = \left(N - (M+1)\right) E_s$ is a constant term, it does not change the set of optimal solutions, hence, it can be ignored from (26). $\tilde{G}_{t_D}$ is the target gram matrix which is chosen from a convex set $\mathcal{H}_{\mu_{welch}}$ as defined in (18). The problem in (26) can be solved using the Algorithm 1 to design the optimal sensing matrix at the second stage. We initialize $\tilde{\boldsymbol{\Phi}}_D$ to a random matrix as used at first stage. After obtaining the optimal design of the sensing matrix $\hat{\boldsymbol{\phi}}_D$, we formulate the NKP problem to design the hybrid precoder/combiner jointly as

$$\begin{aligned}
\{F_{d,n}^{opt}, W_{d,n}^{opt}\} &= \underset{F_{d,n}^{opt}, W_{d,n}^{opt}}{\arg\min} \left\| \hat{\boldsymbol{\phi}}_{d,n} - F_{d,n}^T \otimes W_{d,n}^H \right\|_F \\
&\text{s.t.} \quad \left\| F_{d,n} \otimes W_{d,n} \right\|_F^2 \leq N_{RF}^{\mathtt{tx}} N_{RF}^{\mathtt{rx}}
\end{aligned} \tag{27}$$

In a similar manner, we adopt the added constraint on $F_{d,n}$ and $W_{d,n}$ to satisfy the total power constraints of hybrid systems. For designing the joint hybrid precoding and combining at the second stage, we change the size of each submatrix in $\boldsymbol{\Xi}$ to $N_{RF}^{\mathtt{tx}} N_{RF}^{\mathtt{rx}} \times N_{\mathtt{tx}} N_{\mathtt{rx}}$ in the initialization phase in algorithm 2.

V. MULTI-STAGE COMPRESSED SENSING-BASED CHANNEL ESTIMATION

After the joint design of hybrid precoders and combiners from the optimal sensing matrix, we revisit in this section the multi-stage CS-based algorithm suggested in our previous paper [26] to estimate the mmWave channel. We recall that the multi-stage CS-based algorithm performs explicit sparse channel estimation in the angular domain with limited random pilots and detected data symbols as training beams. Using limited random pilot numbers reduces the effect of the overlapping between training beams which maximizes spatial diversity. Further, using the detected data symbols as training beams improves the performance of CS recovery algorithms by increasing the measurement numbers of sensing matrices. In addition to this, the spectral efficiency (SE) of mmWave MIMO systems is enhanced by exploiting the detected data symbols.

A. FIRST STAGE

To improve the computational complexity of channel estimation at the first stage, we adopt the open-loop approach to accomplish the explicit channel estimation. The system model in (10) represents the CS formulation which allows using the greedy algorithms to estimate the mmWave channel. In our case, we can construct the sensing matrix $\check{\boldsymbol{\Phi}}_P$ to estimate the channel at the first stage by using the joint design of hybrid precoders $\overline{S}^{opt}$ and combiners W^{opt} matrices obtained by the Algorithm 2. The estimation problem of channel h_α can be defined by the following optimization problem

$$\hat{h}_\alpha = \arg\min_{h_\alpha} \left\| \tilde{y}_P - \sqrt{\gamma}\breve{\boldsymbol{\Phi}}_P \boldsymbol{\Psi} h_\alpha \right\|_2 \quad \text{subjet to } \|h_\alpha\|_0 \leqslant L \tag{28}$$

Obviously, the optimization problem in (28) is a non-convex optimization with $\mathcal{L}_0$ norm constraint. Therefore, the finding of its solution will be difficult and intractable. When the signal is sparse in a known basis, we use the orthogonal matching pursuit (OMP) algorithm to estimate the mmWave channel.

B. SECOND STAGE

As mentioned previously, we exploit the estimated channel in the second stage to detect unknown data symbols and exploit it in the next stage as training beams. Although many MIMO detection algorithms have been proposed in the literature. The major challenges of the MIMO detectors are the implementation difficulty and performance issue on the receiver side. When trying to pick the best MIMO detector, we used different detection techniques such as least square (LS), Zero-Forcing (ZF), Minimum mean square error (MMSE), minimum mean-squared error with successive interference cancellation (MMSE-SIC), simplicity [41], and semidefinite relaxation row-by-row (SDR-RBR) [42]. According to the obtained detection results in [26], the SDR-RBR detector achieves high performance with low complexity, especially in the QPSK scenario. Thus, we choose the SDR-RBR detector as a promising MIMO detector in the second stage to detect the unknown data symbols. By considering the $N-(M+1)$ unknown data symbols transmitted via the estimated channel. At each sample transmission, each received data signal of the system model in (11) can be rewritten as

$$y_{d,n} = \sqrt{\gamma}\underbrace{W_{d,n}^H \hat{H} F_{d,n}}_{\boldsymbol{\Theta}_{d,n}} x_{d,n} + \overline{\boldsymbol{\eta}}_{d,n} \quad n = M+1,\ldots,N \tag{29}$$

where $y_{d,n} \in \mathbb{C}^{N_{RF}^{\mathtt{rx}}\times 1}$ denotes the received signal vector at the n^{th} time sample, and $\hat{H}$ is the estimated channel matrix at the first stage. $\overline{\boldsymbol{\eta}}_{d,n}$ indicates the noise vector after combining at $\mathtt{Rx}$.

The MIMO data detection problem to examine all possible signals in the symbol constellation set $\mathcal{X} = \{\pm 1 \pm j\}$ can be expressed as

$$\hat{x}_{d,n} = \arg\min_{x_{d,n}\in\mathcal{X}} \left\| y_{d,n} - \sqrt{\gamma}\,\boldsymbol{\Theta}_{d,n} x_{d,n} \right\|_2. \tag{30}$$

According to the literature on MIMO detectors, the issue in (30) can be resolved by a maximum likelihood (ML) detector to offer the best performance during the second stage of data detection. However, ML detection requires high computational complexity due to exhaustively searching for all the candidate vectors. Moreover, the ML detector can be prohibitively complex even for a small-scale MIMO detection [43]. Therefore, SDR-RBR detector deals with the ML detection problem to reduce the computational complexity, especially when using the BPSK/QPSK modulation.

To apply the SDR-RBR solution, we convert the model in (29) to an equivalent real-valued system as follows

$$y_{c,n} = \sqrt{\gamma}\,\boldsymbol{\Theta}_{c,n} x_{c,n} + \overline{\boldsymbol{\eta}}_{c,n} \tag{31}$$

where $y_{c,n} \in \mathbb{R}^{2N_{RF}^{\mathtt{rx}}\times 1}$ represents the real-valued received signal vector, and $\boldsymbol{\Theta}_{c,n} \in \mathbb{R}^{2N_{RF}^{\mathtt{rx}}\times 2N_{RF}^{\mathtt{tx}}}$ denotes the real-valued matrix version of $\boldsymbol{\Theta}_{d,n}$, whereas $x_{c,n} \in \mathbb{R}^{2N_{RF}^{\mathtt{tx}}\times 1}$ is a real-valued unknown data vector, and $\overline{\boldsymbol{\eta}}_{c,n}$ is a real-valued additive gaussian noise vector. Hence, the SDR problem can be defined by the following formulation

$$\begin{aligned}\hat{x}_{c,n} = &\arg\min_{x_{c,n}\in\mathcal{S}^{2N_{RF}^{\mathtt{rx}}}} \Big\{ \mathrm{Tr}(\boldsymbol{\Theta}_{c,n}^T \boldsymbol{\Theta}_{c,n} X) - 2\boldsymbol{s}_{c,n}^T \boldsymbol{\Theta}_{c,n}^T y_{c,n} \\ &+ \left\| y_{c,n} \right\|_2^2 \Big\}. \\ &\text{subject to} \quad X \succeq x_{c,n}^T \boldsymbol{x}_{c,n} \\ &x_{ii} = 1, i = 1,\ldots,2N_{RF}^{\mathtt{rx}}\end{aligned} \tag{32}$$

For detecting the unknown data symbols, we adopt the row-by-row (RBR) method proposed in [42] to solve this SDR detection problem.

C. LAST STAGE

We exploit random pilots of the first stage, and the detected data symbols in the second stage to construct the sensing matrix $\breve{\boldsymbol{\Phi}}_G$ to form the CS model (8). In the last stage, we refine the re-estimation of the mmWave channel by solving the optimization problem with the following form

$$\tilde{h}_\alpha = \arg\min_{h_\alpha} \left\| \tilde{y}_G - \sqrt{\gamma}\,\breve{\boldsymbol{\Phi}}_G \boldsymbol{\Psi} h_\alpha \right\|_2 \quad \text{subjet to } \|h_\alpha\|_0 \leq L. \tag{33}$$

As established, increasing the measurement set always means better performance. It seems from the last stage, we have more measurements which lead certainly to enhance the recovery process performance of the true support of h_α. Since the measurement numbers increase due to using the detected data as training beams. We exploit the gOMP algorithm to accomplish the mmWave channel re-estimation with fast processing speed and competitive computational complexity [44]. Algorithm 3 summarizes all algorithms that are used in each stage for estimating the mmWave channel.

VI. SIMULATION RESULTS

This section compares the performance of the proposed method for designing the sensing matrix to the outcomes of other methods for designing sensing matrices, such as Renjie's method [38], Elad's method [34], and Hong's

Algorithm 3 Multi-Stage CS-Based mmWave Channel Estimation Using Joint Hybrid Precoding and Combining Design

Initialization: i) $\mathbf{H}$; ii) randomly generation of F/W

First stage : Estimating $\hat{h}_\alpha$

Design $\hat{\boldsymbol{\phi}}_P$ using Algorithm (1)

Design Jointly $\overline{S}^{opt}/W^{opt}$ using Algorithm (2)

Construct $\check{\boldsymbol{\Phi}}_P$ using $\overline{S}^{opt}/W^{opt}$

Formulate the model defined in (10) using $\check{\boldsymbol{\Phi}}_P$

estimate h_α by solving:

$$\begin{cases} \hat{h}_\alpha = \arg\min_{h_\alpha} \left\| \tilde{y}_P - \sqrt{\gamma}\check{\boldsymbol{\Phi}}_P \boldsymbol{\Psi} h_\alpha \right\|_2 \\ \text{subjet to } \|h_\alpha\|_0 \leq L \end{cases} \triangleright \text{ using OMP}$$

Second stage: Detecting $\hat{x}_{d,n}$

Input $\hat{H}$, Construct $\tilde{\boldsymbol{\Phi}}_D$ randomly generation of F_D/W_D

Design $\hat{\boldsymbol{\phi}}_D$ using Algorithm (1)

Design jointly F_D^{opt}, W_D^{opt} using Algorithm (2)

for $M+1 \leqslant n \leqslant \boldsymbol{N}$ *do*

Training $F_{d,n}^{opt}$, $W_{d,n}^{opt}$

$\forall\, n: \; y_{c,n} = \sqrt{\gamma}\boldsymbol{\Theta}_{c,n} s_{c,n} + \boldsymbol{\overline{\eta}}_{c,n}$

Detection $x_{c,n}$ by solving problem in (32) $\triangleright$ using SDR-RBR

end for

Last stage: Re-estimating $\tilde{h}_\alpha$

Construct $\check{\boldsymbol{\Phi}}_G$ using $\overline{S}^{opt}/W^{opt}$ and F_D^{opt}, W_D^{opt}

Formulate the model defined in (8)

re-estimate h_α by solving:

$$\begin{cases} \tilde{h}_\alpha = \arg\min_{h_\alpha} \left\| \tilde{y}_G - \sqrt{\gamma}\check{\boldsymbol{\Phi}}_G \boldsymbol{\Psi} h_\alpha \right\|_2 \\ \text{subjet to } \|h_\alpha\|_0 \leq L \end{cases} \triangleright \text{ using gOMP}$$

method [33]. We illustrate the simulation results of the mutual coherence values minimizing obtained by the proposed method. Then, utilizing the suggested joint hybrid precoding and combining design, we evaluate the performance of each stage that is used to estimate the mmWave channel according to the multi-stage CS technique. In this study, simulations were run without regard to established standards. In addition to using a single carrier modulation in the simulations, all developed techniques are processed in the time domain.

A. PERFORMANCE OF MINIMIZING THE MUTUAL COHERENCE VALUES

In this subsection, we provide the performance of mutual coherence values as measure metrics to evaluate the quality of the designed sensing matrix over 40 outer iterations, where the given dictionary matrix $\boldsymbol{\Psi} \in \mathbb{R}^{80\times 120}$ is a random Gaussian matrix and $\boldsymbol{\Phi} \in \mathbb{R}^{28\times 80}$ is generated randomly as the initial matrix. For Elad's method [34], the parameter t is set to 0.2 with three different values of γ: $\gamma_1 = 0.25, \gamma_2 = 0.55, \gamma_3 = 0.95$. The parameters ζ and inner iteration number for Hong's method [33] are set to μ_{welch} and 2, respectively, with the normalization of the equivalent dictionary $\mathbf{D}$ during each iteration. Due to the absence of an analytical solution for choosing the suitable parameter c to establish the thresholding of the shrinkage function, c is set to 0.01 for Renjie's method [38] with the same sizes of the sensing matrix $\boldsymbol{\Phi}$ and dictionary $\boldsymbol{\Psi}$ used in [38]. Fig.2 shows the evolution results of mutual coherence values versus outer iteration numbers. According to this figure, the mutual coherence values corresponding to each method decrease with different convergence speeds. Moreover, it is depicted in Fig.2 (a), (b), and (c) that the proposed method for designing the sensing matrix has a better and more significant evolution in the decrease of the mutual coherence values (μ_{mx}, μ_{ave} and μ_{all}) simultaneously with a simple shrinkage function to update the target Gram matrix $\tilde{G}_t$. Reconstruction performance analyses of the proposed sensing matrix design for CS framework will be studied in future work.

TABLE 1. Computational complexity comparison of different methods used to design the matrix sensing.

Method	Located complexity	Complexity
Hong's method [33]	3, 12, 13, 15, 19, 20	$\mathcal{O}(ItermL^2)$
Elad's method [34]	1,2,5,7	$\mathcal{O}(IterL^3)$
Renjie's method [38]	1,2,4,7	$\mathcal{O}(IterL^3)$
Proposed method	2,3,5,6,7	$\mathcal{O}(IterL^3)$

To analyze the complexity of the sensing matrix design algorithm, we assume that $\boldsymbol{\Phi}$ and $\boldsymbol{\Psi}$ have the size $m \times n$ and $n \times L$ respectively. The table 1 presents the computational complexity to design the sensing matrix by the proposed method compared with Elad's method [34], Hong's method [33], and Renjie's method [38]. As mentioned above, the algorithm is based on an iterative approach. The main computational complexity of algorithm 1 in each iteration lies in calculating the complexity functions at steps 2, 3, 5, 6, and 7. Therefore, the flops required for those steps are $\mathcal{O}(mnL)$, $\mathcal{O}(mL^2)$, $\mathcal{O}(L^3)$, and $\mathcal{O}(n^3)$ respectively. The computational complexity of algorithm 1 is equal to $\mathcal{O}(IterL^3)$. From the table 1, it seems that Hong's method [33] reduces slightly the complexity of the sensing matrix design. On the other hand, the proposed algorithm designs the sensing matrix with affordable computation and better performance in terms of decreasing the mutual coherence values (μ_{mx}, μ_{ave} and μ_{all}) simultaneously.

B. PERFORMANCE COMPARISON OF MMWAVE CHANNEL ESTIMATION

We present in this subsection the simulation results of the proposed joint hybrid precoder and combiner design used to estimate the mmWave channel according to the multi-stage CS approach [26]. Indeed, we compare the performance of the proposed method with the results of the existing methods that are based on codebook schemes. In our simulations, the $\mathtt{Tx}$ and the $\mathtt{Rx}$ are equipped with $N_{\mathtt{tx}} = N_{\mathtt{rx}} = 32$ antennas arranged in ULA configuration with spacing between antenna elements equal to $\frac{\lambda}{2}$. The analog part at each

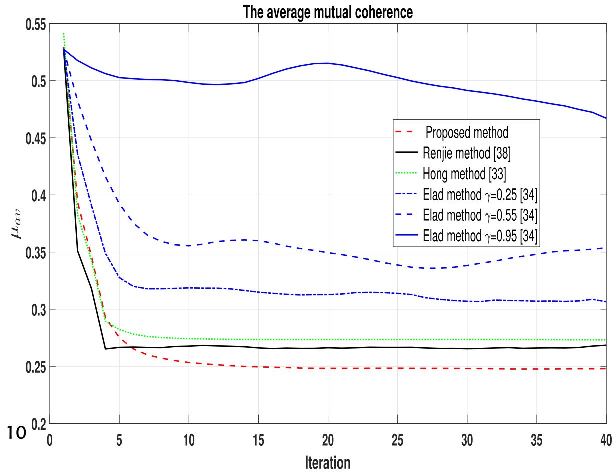

(a)

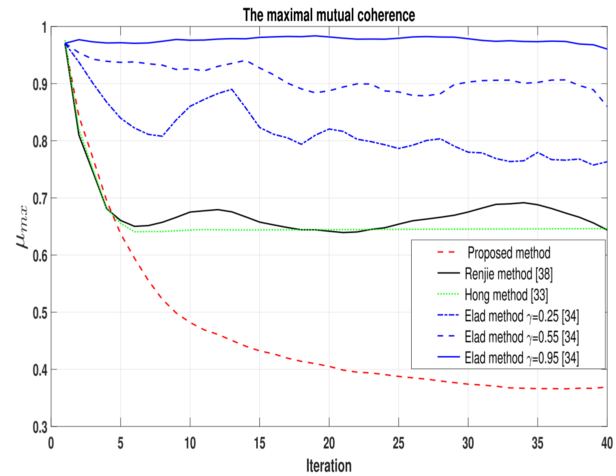

(b)

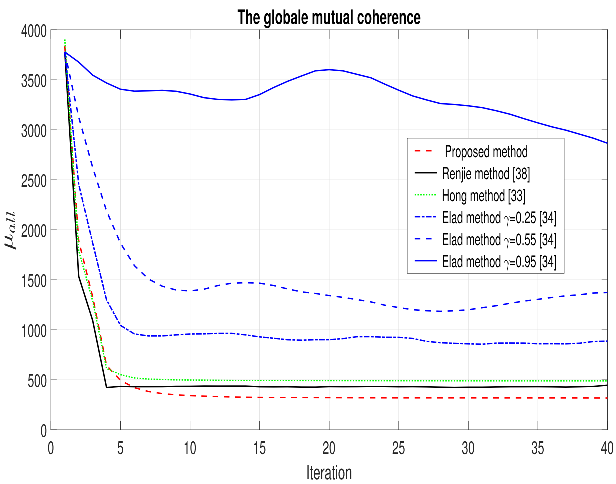

(c)

FIGURE 2. Evolution results of: (a) the t-averaged mutual coherence μ_{ave}, (b) the maximal coherence μ_{mx}, and (c) the global mutual coherence μ_{all}, all versus iteration number for an 28 × 80 random matrix Φ as initial matrix and an 80 × 120 dictionary matrix Ψ with Gaussian distribution.

side is implemented using analog phase shifters as depicted in Fig.1, where the number of RF chains at both $\mathtt{Tx}$ and $\mathtt{Rx}$ are $N_{RF}^{\mathtt{tx}} = N_{RF}^{\mathtt{rx}} = 2$. As mentioned above, we assume that $N_s = 2$ data streams per transmission for ensuring the effectiveness of multiple-stream communications. According to the Saleh-Valenzuela model in (2), the mmWave channel is generated with $L = 9$ paths that folllow the Rayleigh distribution. However, the AoA/AoD azimuth angles of each path are random and uniformly distributed over $[0, 2\pi]$. We assume that the mmWave transceiver operates at 28 GHz with transmission bandwidth $\boldsymbol{B}_w = 500$ MHz [45], where the noise power can be written as $\sigma = -174 + 10\log_{10}(\boldsymbol{B}_w)$. As power allocation methods increase the mmWave architecture complexity due to the use of power amplifiers (PAs). The same total power constraint is adopted throughout the simulation with equal power allocation at each n^{th} time sample as presented in equation (1). Hence, we can define the SNR as γ/σ. The performance of the proposed method is evaluated via the SE and the normalized mean squared error (NMSE) that is defined as $\mathbb{E}[\left\| H - \hat{H} \right\|_F^2 / \|H\|_F^2]$, where $\mathbf{H}$ and $\hat{H}$ are the true channel and the estimated channel, respectively. As mentioned above, to formulate the CS reconstruction model according to the VAD representation, we use $G = 100$ as number of angle grids at the tranceiver for generating the overcomplete dictionary matrix $\boldsymbol{\Psi}$. The hybrid training precoders/combiners of each transmitted sample are randomly generated using 6 quantization bits to design RF phase shifters to realize analog beamformers/combiners. The outer iteration numbers used in algorithm 1 equal 2 for designing the optimal sensing matrix at the first and second stages. For estimating the mmWave channel at the first stage, random pilot numbers are set to 250. While we exploit the symbol error rate (SER) performance comparison to evaluate the detection of the unknown transmitted data at the second stage by exploiting the QPSK modulation due to its low error probability results.

Fig. 3 depicts NMSE performance versus SNR using the proposed joint hybrid precoder and combiner design, and the method random design [26] for estimating the mmWave channel via OMP, Oracle, and LS estimators. The NMSE results of LS estimator with the random design method proposed in [26] (LS-RD estimator) are lower compared to the others due to the underdetermination of the received training signal model in (10) that raised from the fewer measurement numbers than the product of $N_{\mathtt{tx}}$ and $N_{\mathtt{rx}}$ in the construction of the sensing matrix $\boldsymbol{\Phi}_P$ at the first stage. In addition, the use of LS estimator in sparsity recovery needs more measurements to obtain the highest results regardless of the matrix sensing quality. In general, the oracle estimator can be exploited as a lower bound to evaluate the estimation performance due to the prior knowledge of AoDs/AoAs that correspond to the true dominant paths. The oracle estimator with the proposed joint hybrid design (Oracle-JD estimator) provides the best NMSE performance than the oracle estimator with random hybrid design in [26] (Oracle-RD estimator). For the OMP algorithm performance, the results obtained with the proposed joint hybrid design

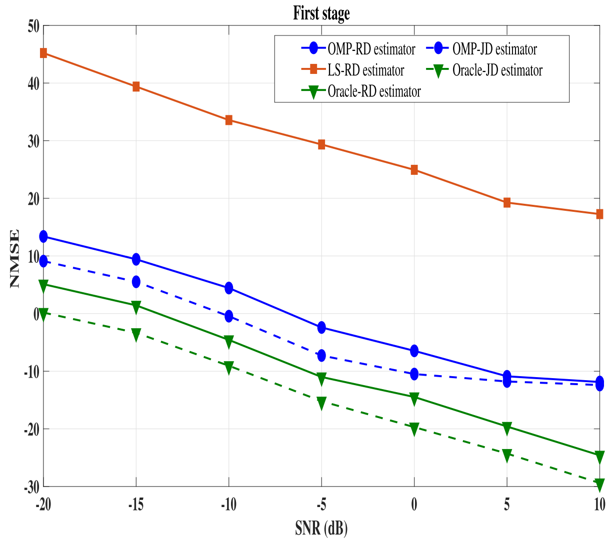

FIGURE 3. NMSE performance of mmWave channel estimation at first stage vs. SNR with the proposed joint design method, the method random design [26] by using OMP, Oracle and LS algorithms.

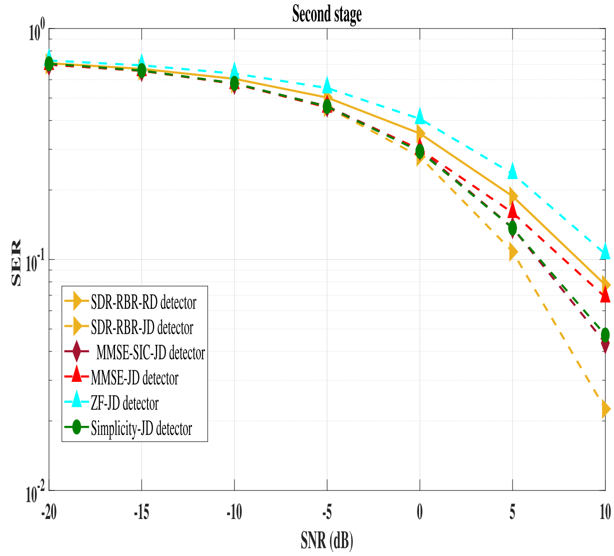

FIGURE 4. SER performance results vs. SNR of the ZF-JD, MMSE-JD, MMSE-SIC-JD, Simplicity-JD, SDR-RBR-JD with the proposed joint hybrid design and SDR-RBR-RD with the random hybrid design proposed in [26] at the second stage.

(OMP-JD estimator) has significant superiority compared to random hybrid design in [26](OMP-RD estimator), especially in the low SNR regime. From this figure, the results of estimator algorithms obtained by using the proposed joint hybrid design achieve the best performance due to the smaller mutual coherence of the equivalent dictionary which contributes to enhance and improve the channel estimation accuracy. According to the multi-stage CS approach, we use the estimated channels provided by the proposed method and the method proposed in [26] at the first stage to send and detect the unknown data. Fig. 4 compares the SER performance of various detection techniques (ZF-JD, MMSE-JD, MMSE-SIC-JD, Simplicity-JD, SDR-RBR-JD) by using the proposed joint hybrid design and the results of SDR-RBR detector with the random hybrid design proposed in [26] (SDR-RBR-RD).

As depicted in Fig. 4, from the $SNR - 10dB$, we can find that the SER performance gap between the SDR-RBR-JD and SDR-RBR-RD enlarges noticeably and strikingly with the increasing of SNR values. In particular, as proven in [26], the use of SDR-RBR-based detector can achieve the best results for hybrid MIMO architecture when the data are transmitted via QPSK modulation. Thanks to the proposed joint design, the orthogonality of the spatial multiplex channel is guaranteed for reducing the effect of inter-symbol interference (ISI) on the performance of the SER. Therefore, using the MMSE, MMSE-SIC, and Simplicity algorithms with the proposed joint hybrid design in the detection process can produce better SER performance compared with the result of the SDR-RBR-RD detector. Further, the high accuracy of channel estimation at the first stage by the proposed method improves also the detection results. Utilizing detected data as training beams ensures spatial diversity by lowering the overlapping effect and expanding the measurement set, which in turn increases the accuracy of mmWave channel estimation without any correlation between the training beams. This thus results in improved communication performance. Therefore, the detected data symbols using the semidefinite relaxation (SDR) algorithms (SDR-RBR-RD, SDR-RBR-JD) are re-used as beam training to re-estimate the channel again at the last stage. Fig. 5 shows the NMSE performance and results of mmWave channel estimation at the last stage by the suggested joint design method, the method random design [26] via gOMP and Oracle algorithms using $G = 100$ compared with other methods based on codebook schemes by using $G = 160$ as codebook based minimal total coherence (MTC) scheme [23], codebook based ordering scheme [24], codebook based Versatile scheme [25], codebook based random scheme.

As depicted in Fig. 5, the oracle estimator with the proposed joint hybrid design (Oracle-JD estimator) achieve better results in term of the NMSE performance compared with the results obtained by all the other methods. The gOMP estimator with the proposed joint hybrid design (gOMP-JD estimator) has the same NMSE performance as the obtained results by methods based on codebook schemes at the low SNR range although the use of high grid size by those methods, whereas, from SNR 0 dB, the gOMP-JD estimator shows good outcomes compared to codebook-based schemes with a similar trend to oracle estimators performance.

The Fig. 6 represents the achieved SE by the precoding and combining matrices derived from the SVD decomposition of mmWave channel which is estimated by the proposed joint hybrid method and random hybrid method [26], codebook-based minimal total coherence

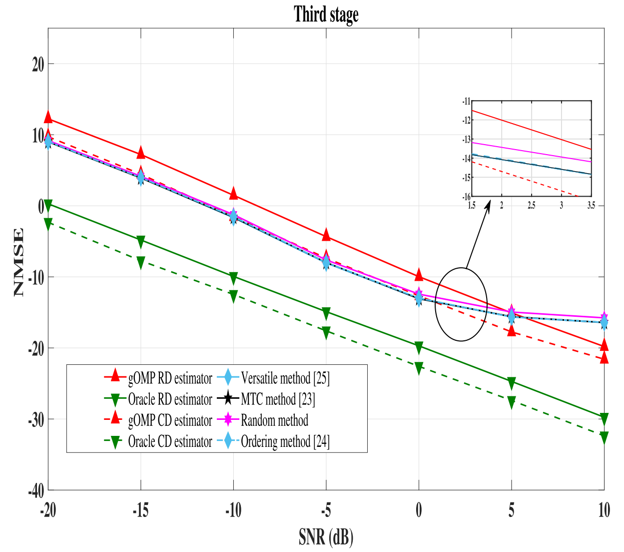

FIGURE 5. NMSE performance results of mmWave channel estimation at the third stage vs. SNR of the proposed joint design method, the method random design [26] via gOMP, Oracle algorithms by using $G = 100$ compared with other methods based on codebook schemes by using $G = 160$ as codebook based minimal total coherence (MTC) scheme [23], codebook based ordering scheme [24], codebook based Versatile scheme [25], codebook based random scheme.

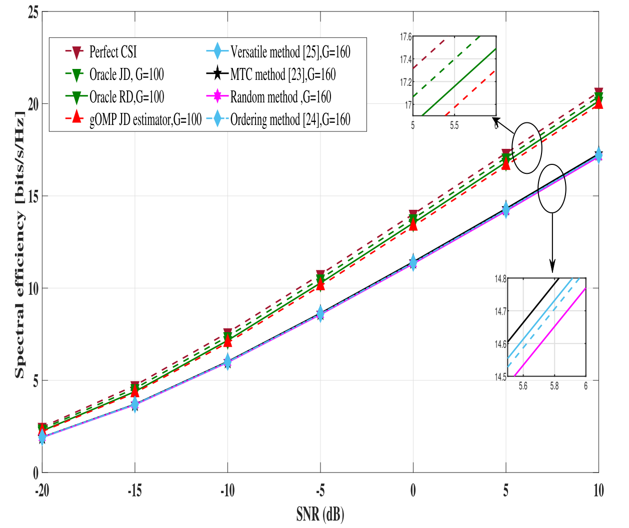

FIGURE 6. SE comparison with the varying SNR using SVD decomposition to derive the precoders and combiners from of mmWave channel matrices estimated by different methods.

TABLE 2. Computational complexity comparison of algorithm 3.

Operation	Online complexity	Offline complexity
First stage: Sensing matrix design: $\mathcal{O}(IterG^3)$ Joint hybrid design: $\mathcal{O}(2N_{RF}^{\mathtt{tx}}N_{\mathtt{tx}}N_{\mathtt{rx}}M)$ Estimate h_α: $\mathcal{O}(LMG^2)$ **Second stage**: Sensing matrix design: $\mathcal{O}(IterG^3)$ Joint hybrid design: $\mathcal{O}(2N_{RF}^{\mathtt{tx}}N_{\mathtt{tx}}N_{\mathtt{rx}}(N-M-1))$ Data detection : $\mathcal{O}((2N_{RF}+1)^3(N-M-1))$ **Third stage**: Re-estimate $\tilde{\mathbf{h}}_\alpha$: $\mathcal{O}(NG^2)$	$\mathcal{O}(IterG^3)$	$\mathcal{O}(LMG^2)$

(MTC) scheme [23], codebook-based ordering scheme [24], codebook-based Versatile scheme [25], and codebook based-random scheme. The obtained SE using the perfect CSI can be considered as the upper bound in the comparison. According to this figure, the oracle algorithm with the proposed joint hybrid design and random hybrid design [26] reach a better performance than the others. On the other hand, the gOMP algorithm with the proposed joint hybrid design has best results than the codebook-based schemes. The achieved high SE of the proposed joint hybrid design is obtained thanks the high channel estimation accuracy by taking into account the multiplexing system factor during the design of hybrid precoders and combiners process. Moreover, the SE of mmWave MIMO systems is enhanced by exploiting the detected data symbols.

For evaluating the computational complexity of algorithm 3, we analyze the complexity of the used algorithm and method at each stage to achieve the task of sensing matix design, estimation, detection, and re-estimation. At the first stage, we designed the sensing matrix using algorithm 1 where this step has a complexity of $\mathcal{O}(IterG^3)$. After that, we jointly designed the hybrid precoder and hybrid combiner thanks to algorithm 2 which has the complexity of $\mathcal{O}(2N_{RF}^{\mathtt{tx}}N_{\mathtt{tx}}N_{\mathtt{rx}}M)$. The estimation channel step is performed by the OMP algorithm, thus the complexity of this task is about $\mathcal{O}(LMG^2)$, where L is the number of paths, M indicates the number of pilots, and G is the number of angle grids used in our simulation. Then, the complexity of the sensing matrix design is $\mathcal{O}(IterG^3)$ at the second stage, and with its parameters, the computational complexity of the joint design method is $\mathcal{O}(2N_{RF}^{\mathtt{tx}}N_{\mathtt{tx}}N_{\mathtt{rx}}(N-M-1))$. As mentioned above, we adopted the SDR-RBR detector to reduce the complexity and perform the detection results. For the detection process, the complexity of row-by-row (RBR) method is $\mathcal{O}((2N_{RF}+1)^3(N-M-1))$. The last stage is concretized by the gOMP algorithm with a complexity of $\mathcal{O}(NG^2)$. From table 2, the computational complexity of algorithm 3 has the same computational load as the sensing matrix design complexity which is proportional to G^3. To reduce the complexity of algorithm 3, we can perform both the sensing matrix design and derive the joint hybrid separately before executing algorithm 3 as used in the design of the Grassmannian codebook for mmWave MIMO communication systems. Therefore, the complexity of the proposed method can be expressed by the complexity of the OMP algorithm where its complexity depends on the grid size. From the simulation parameters, the offline complexity of the proposed method is less than the complexity of the proposed methods in [23],

[24], [25], and [26] because the proposed method requires less grid size to achieve better performance as verified by the simulation comparison.

VII. CONCLUSION

In this paper, we proposed a new joint hybrid precoders and combiners design to improve the mmWave multiplexing system which also ensures the spatial diversity. As the small mutual coherence of the sensing matrix does not contribute to guaranteeing the high-performance results of CS-based mmWave channel estimation algorithms, we propose a new iterative method based on alternating minimization to design the optimal sensing matrix with the given dictionary for minimizing the mutual coherence values simultaneously according to ETF properties. Then, we exploit this optimally to derive jointly the hybrid precoders and combiners simultaneously for each transmitted sample by using the NKP problem as an optimization design problem. The evolution results of mutual coherence values versus outer iteration numbers demonstrated that the proposed sensing matrix design has a better and more significant evolution in terms of decreasing the mutual coherence values (μ_{mx}, μ_{ave} and μ_{all}) simultaneously with the simple shrinkage function. Also, the proposed joint hybrid design produces high mmWave channel estimation accuracy and achieves the best results in terms of SE performance.

APPENDIX A

Proof of theorem (1)

To design the optimal sensing matrix, the objective function can be expressed in general manner as

$$f = \left\| \tilde{G}_t - \mathbf{\Psi}^H \mathbf{\Phi}^H \mathbf{\Phi} \mathbf{\Psi} \right\|_F^2 \tag{34}$$

Let $\mathbf{\Psi} = U_\Psi \Sigma_\Psi V_\Psi^H$ the SVD decomposition of $\mathbf{\Psi}$. f can be rewritten as

$$f = \left\| \tilde{G}_t - V_\Psi \mathbf{\Sigma}_\Psi^H U_\Psi^H \mathbf{\Phi}^H \mathbf{\Phi} U_\Psi \mathbf{\Sigma}_\Psi V_\Psi^H \right\|_F^2 \tag{35}$$

By suggesting that

$$M = \mathbf{\Phi} U_\Psi \mathbf{\Sigma}_\Psi \tag{36}$$

So the function in (35) can be expressed as

$$f = \left\| \tilde{G}_t - V_\Psi M^H M V_\Psi^H \right\|_F^2 \tag{37}$$

As V_Ψ is orthonormal matrix. The Frobenius norm expression can be written by using linearity and cyclic properties of trace as:

$$f = \left\| V_\Psi^H \tilde{G}_t V_\Psi - M^H M \right\|_F^2 \tag{38}$$

We denote $\mathbf{\Theta} = V_\Psi^H \tilde{G}_t V_\Psi$

$$f = \left\| \mathbf{\Theta} - M^H M \right\|_F^2 \tag{39}$$

if $\mathbf{\Theta} = V_\Psi^H \tilde{G}_t V_\Psi$ is a positive semidefinite matrix, then $\mathbf{\Theta} = X_\Theta A_\Theta {X_\Theta}^H$ be the eigendecomposition of $\mathbf{\Theta}$ where $X_\Theta \in \mathbb{C}^{n\times n}$ is orthonormal matrix, and A_Θ is the diagonal matrix which contains the eigenvalues of $\mathbf{\Theta}$

$$f = \left\| X_\Theta A_\Theta {X_\Theta}^H - M^H M \right\|_F^2 \tag{40}$$

By using linearity and cyclic property of trace, we can get

$$f = \left\| A_\Theta - {X_\Theta}^H M^H \boldsymbol{M} X_\Theta \right\|_F^2 \tag{41}$$

To get the minimum value of (39), $\mathbf{\Theta} = M^H M$, therefore $M^H M$ eigenvalues decomposition have the same orthonormal basis of $\mathbf{\Theta}$ according to the spectral theorem [46]. Thereby, there exist unitary matix X_Θ such that

$${X_\Theta}^H M^H M X_\Theta = \mathbf{\Lambda}_\Theta = \begin{bmatrix} \mathbf{\Lambda}_{\Theta_m} & 0 \\ 0 & 0 \end{bmatrix} \tag{42}$$

$\mathbf{\Lambda}_{\Theta_m} \neq 0$ if $rank(M^H M) = min(m, n)$, so that the objective function in (41) becomes

$$f = \left\| A_\Theta - \begin{bmatrix} \mathbf{\Lambda}_{\Theta_m} & 0 \\ 0 & 0 \end{bmatrix} \right\|_F^2 \tag{43}$$

To get the minimum in (43), $A_\Theta = \begin{bmatrix} \mathbf{\Lambda}_{\Theta_m} & 0 \\ 0 & 0 \end{bmatrix}$. Therefore $M^H M = X_\Theta \begin{bmatrix} \mathbf{\Lambda}_{\Theta_m} & 0 \\ 0 & 0 \end{bmatrix} {X_\Theta}^H = P_{n\times m} \mathbf{\Lambda}_{\Theta_m} P_{n\times m}^H$, where $\boldsymbol{P}_{n\times m}$ is the matrix that contains the eigenvectors corresponding to the non-zero eigenvalues. $\mathbf{\Lambda}_{\Theta_m}$ can be writing as $\mathbf{\Lambda}_{\Theta_m} = \mathbf{\Lambda}_{\Theta_m}^{1/2} \mathbf{\Lambda}_{\Theta_m}^{1/2}$

As eigenvaules matrix is a symmetric matrix, $\boldsymbol{M}$ can be defined as

$$M = \mathbf{\Lambda}_{\Theta_m}^{1/2} \boldsymbol{P}_{n\times m}^H \tag{44}$$

By substituting (44) in (36), we can find $\mathbf{\Phi} U_\Psi \mathbf{\Sigma}_\Psi = \mathbf{\Lambda}_{\Theta_m}^{1/2} P_{n\times m}^H$

In the end, we get $\mathbf{\Phi}_1 = \mathbf{\Lambda}_{\Theta_m}^{1/2} P_{n\times m}^H \left[\mathbf{\Sigma}_\Psi^{-1} \; 0 \right]^H U_\Psi^H$

APPENDIX B

Proof of Lemma (3)

Let the squared Frobenius norm of matrix $\mathbf{\Gamma}$ is given by

$$\|\mathbf{\Gamma}\|_F^2 = \mathrm{Tr}(\mathbf{\Gamma}\mathbf{\Gamma}^H)$$

by using the kronecker product properties, we can get

$$\begin{aligned} &= \mathrm{Tr}((z \otimes \mathbf{\Gamma})(z \otimes \mathbf{\Gamma})^H) \\ &= \mathrm{Tr}(\underbrace{zz^H}_{A} \otimes \underbrace{\mathbf{\Gamma}\mathbf{\Gamma}^H}_{B}) \\ &= \mathrm{Tr}(A \otimes B) \end{aligned}$$

where $A, B \in \mathbb{C}^{m\times m}$ are square matrices, by applying the Cauchy-Schwarz inequality and matrix trace rule, we can obtain

$$\|A \otimes B\|_F^2 \leq \mathrm{Tr}(A)\mathrm{Tr}(B) \tag{45}$$

where Tr stands for a matrix trace, the inequality in (45) can be rewritten as

$$\|A \otimes B\|_F^2 \leq \|A\|_F^2 \, \|B\|_F^2 \tag{46}$$

when $\|A\|_F^2 = 1$, the last inequality can be represented as

$$\|A \otimes B\|_F^2 \leq \|B\|_F^2 \tag{47}$$

REFERENCES

[1] T. S. Rappaport, Y. Xing, G. R. MacCartney, A. F. Molisch, E. Mellios, and J. Zhang, "Overview of millimeter wave communications for fifth-generation (5G) wireless networks—With a focus on propagation models," *IEEE Trans. Antennas Propag.*, vol. 65, no. 12, pp. 6213–6230, Dec. 2017.

[2] W. Ma, C. Qi, and G. Y. Li, "High-resolution channel estimation for frequency-selective mmWave massive MIMO systems," *IEEE Trans. Wireless Commun.*, vol. 19, no. 5, pp. 3517–3529, May 2020.

[3] C.-R. Tsai and A.-Y. Wu, "Structured random compressed channel sensing for millimeter-wave large-scale antenna systems," *IEEE Trans. Signal Process.*, vol. 66, no. 19, pp. 5096–5110, Oct. 2018.

[4] Z. Zhang, X. Wu, and D. Liu, "Joint precoding and combining design for hybrid beamforming systems with subconnected structure," *IEEE Syst. J.*, vol. 14, no. 1, pp. 184–195, Mar. 2020.

[5] R. W. Heath Jr., N. González-Prelcic, S. Rangan, W. Roh, and A. M. Sayeed, "An overview of signal processing techniques for millimeter wave MIMO systems," *IEEE J. Sel. Topics Signal Process.*, vol. 10, no. 3, pp. 436–453, Apr. 2016.

[6] M. R. Castellanos, V. Raghavan, J. H. Ryu, O. H. Koymen, J. Li, D. J. Love, and B. Peleato, "Channel-reconstruction-based hybrid precoding for millimeter-wave multi-user MIMO systems," *IEEE J. Sel. Topics Signal Process.*, vol. 12, no. 2, pp. 383–398, May 2018.

[7] A. Morsali, A. Haghighat, and B. Champagne, "Deep learning framework for hybrid analog-digital signal processing in mmWave massive-MIMO systems," 2021, *arXiv:2107.14704*.

[8] A. Banerjee, K. Vaesen, A. Visweswaran, K. Khalaf, Q. Shi, S. Brebels, D. Guermandi, C.-H. Tsai, J. Nguyen, and A. Medra, "Millimeter-wave transceivers for wireless communication, radar, and sensing," in *Proc. IEEE Custom Integr. Circuits Conf. (CICC)*, Apr. 2019, pp. 1–11.

[9] M. Cui, W. Zou, Y. Wang, and R. Zhang, "Low complexity joint hybrid precoding algorithm for millimeter wave MIMO systems," *IEEE Access*, vol. 6, pp. 56423–56432, 2018.

[10] D. H. N. Nguyen, L. B. Le, T. Le-Ngoc, and R. W. Heath Jr., "Hybrid MMSE precoding and combining designs for mmWave multiuser systems," *IEEE Access*, vol. 5, pp. 19167–19181, 2017.

[11] J. G. Andrews, T. Bai, M. N. Kulkarni, A. Alkhateeb, A. K. Gupta, and R. W. Heath Jr., "Modeling and analyzing millimeter wave cellular systems," *IEEE Trans. Commun.*, vol. 65, no. 1, pp. 403–430, Jan. 2017.

[12] X. Gao, L. Dai, S. Han, and R. W. Heath Jr., "Energy-efficient hybrid analog and digital precoding for mmWave MIMO systems with large antenna arrays," *IEEE J. Sel. Areas Commun.*, vol. 34, no. 4, pp. 998–1009, Apr. 2016.

[13] X. Sun and C. Qi, "Codeword selection and hybrid precoding for multiuser millimeter-wave massive MIMO systems," *IEEE Commun. Lett.*, vol. 23, no. 2, pp. 386–389, Feb. 2019.

[14] K. Hassan, M. Masarra, M. Zwingelstein, and I. Dayoub, "Channel estimation techniques for millimeter-wave communication systems: Achievements and challenges," *IEEE Open J. Commun. Soc.*, vol. 1, pp. 1336–1363, 2020.

[15] C. Qi, P. Dong, W. Ma, H. Zhang, Z. Zhang, and G. Y. Li, "Acquisition of channel state information for mmWave massive MIMO: Traditional and machine learning-based approaches," *Sci. China Inf. Sci.*, vol. 64, no. 8, pp. 1–16, Aug. 2021.

[16] S. H. Lim, S. Kim, B. Shim, and J. W. Choi, "Efficient beam training and sparse channel estimation for millimeter wave communications under mobility," *IEEE Trans. Commun.*, vol. 68, no. 10, pp. 6583–6596, Oct. 2020.

[17] Z. Xiao, T. He, P. Xia, and X.-G. Xia, "Hierarchical codebook design for beamforming training in millimeter-wave communication," *IEEE Trans. Wireless Commun.*, vol. 15, no. 5, pp. 3380–3392, May 2016.

[18] A. Alkhateeb, O. E. Ayach, G. Leus, and R. W. Heath Jr., "Channel estimation and hybrid precoding for millimeter wave cellular systems," *IEEE J. Sel. Topics Signal Process.*, vol. 8, no. 5, pp. 831–846, Oct. 2014.

[19] S. Noh, M. D. Zoltowski, and D. J. Love, "Multi-resolution codebook based beamforming sequence design in millimeter-wave systems," in *Proc. IEEE Global Commun. Conf. (GLOBECOM)*, Dec. 2015, pp. 1–6.

[20] B. Hadji, L. Fergani, and M. Djeddou, "Channel estimation based on low-complexity hierarchical codebook design for millimeter-wave MIMO systems," *Int. J. Commun. Syst.*, vol. 34, no. 4, p. e4703, Mar. 2021.

[21] B. Wang, L. Dai, Z. Wang, N. Ge, and S. Zhou, "Spectrum and energy-efficient beamspace MIMO-NOMA for millimeter-wave communications using lens antenna array," *IEEE J. Sel. Areas Commun.*, vol. 35, no. 10, pp. 2370–2382, Oct. 2017.

[22] R. Méndez-Rial, C. Rusu, N. González-Prelcic, and R. W. Heath Jr., "Dictionary-free hybrid precoders and combiners for mmWave MIMO systems," in *Proc. IEEE 16th Int. Workshop Signal Process. Adv. Wireless Commun. (SPAWC)*, Jun. 2015, pp. 151–155.

[23] J. Lee, G.-T. Gil, and Y. H. Lee, "Channel estimation via orthogonal matching pursuit for hybrid MIMO systems in millimeter wave communications," *IEEE Trans. Commun.*, vol. 64, no. 6, pp. 2370–2386, Jun. 2016.

[24] J. Sung and B. L. Evans, "Hybrid beamformer codebook design and ordering for compressive mmWave channel estimation," in *Proc. Int. Conf. Comput., Netw. Commun. (ICNC)*, Feb. 2020, pp. 914–919.

[25] J. Sung and B. L. Evans, "Versatile compressive mmWave hybrid beamformer codebook design framework," in *Proc. Int. Conf. Comput., Netw. Commun. (ICNC)*, Feb. 2020, pp. 1052–1057.

[26] B. Hadji, A. Aïssa-El-Bey, L. Fergani, and M. Djeddou, "Channel estimation using multi-stage compressed sensing for millimeter wave MIMO systems," in *Proc. IEEE 93rd Veh. Technol. Conf. (VTC-Spring)*, Apr. 2021, pp. 1–5.

[27] M. Li, Z. Wang, X. Tian, and Q. Liu, "Joint hybrid precoder and combiner design for multi-stream transmission in mmWave MIMO systems," *IET Commun.*, vol. 11, no. 17, pp. 2596–2604, Nov. 2017.

[28] Z. Wang, M. Li, X. Tian, and Q. Liu, "Joint hybrid precoder and combiner design for mmWave spatial multiplexing transmission," 2017, *arXiv:1704.07988*.

[29] C.-R. Tsai, Y.-H. Liu, and A.-Y. Wu, "Efficient compressive channel estimation for millimeter-wave large-scale antenna systems," *IEEE Trans. Signal Process.*, vol. 66, no. 9, pp. 2414–2428, May 2018.

[30] H. Tang, X. Zhang, H. Chen, L. Zhu, X. Wang, and X. Li, "Incoherent dictionary learning method based on unit norm tight frame and manifold optimization for sparse representation," *Math. Problems Eng.*, vol. 2016, pp. 1–10, 2016.

[31] J. M. Duarte-Carvajalino and G. Sapiro, "Learning to sense sparse signals: Simultaneous sensing matrix and sparsifying dictionary optimization," *IEEE Trans. Image Process.*, vol. 18, no. 7, pp. 1395–1408, Jul. 2009.

[32] V. Abolghasemi, S. Ferdowsi, and S. Sanei, "A gradient-based alternating minimization approach for optimization of the measurement matrix in compressive sensing," *Signal Process.*, vol. 92, no. 4, pp. 999–1009, Apr. 2012.

[33] T. Hong, H. Bai, S. Li, and Z. Zhu, "An efficient algorithm for designing projection matrix in compressive sensing based on alternating optimization," *Signal Process.*, vol. 125, pp. 9–20, Aug. 2016.

[34] M. Elad, "Optimized projections for compressed sensing," *IEEE Trans. Signal Process.*, vol. 55, no. 12, pp. 5695–5702, Dec. 2007.

[35] R. Ramu Naidu and C. R. Murthy, "Construction of unimodular tight frames for compressed sensing using majorization-minimization," *Signal Process.*, vol. 172, Jul. 2020, Art. no. 107516.

[36] E. V. Tsiligianni, L. P. Kondi, and A. K. Katsaggelos, "Construction of incoherent unit norm tight frames with application to compressed sensing," *IEEE Trans. Inf. Theory*, vol. 60, no. 4, pp. 2319–2330, Apr. 2014.

[37] M. A. Sustik, J. A. Tropp, I. S. Dhillon, and R. W. Heath Jr., "On the existence of equiangular tight frames," *Linear Algebra Appl.*, vol. 426, nos. 2–3, pp. 619–635, Oct. 2007.

[38] R. Yi, C. Cui, B. Wu, and Y. Gong, "A new method of measurement matrix optimization for compressed sensing based on alternating minimization," *Mathematics*, vol. 9, no. 4, p. 329, Feb. 2021.

[39] J. A. Tropp, I. S. Dhillon, R. W. Heath Jr., and T. Strohmer, "Designing structured tight frames via an alternating projection method," *IEEE Trans. Inf. Theory*, vol. 51, no. 1, pp. 188–209, Jan. 2005.

[40] C. F. Van Loan and N. Pitsianis, "Approximation with Kronecker products," in *Linear Algebra for Large Scale and Real-Time Applications*. Cham, Switzerland: Springer, 1993, pp. 293–314.

[41] Z. Hajji, K. Amis, and A. A. E. Bey, "Iterative receivers for large-scale MIMO systems with finite-alphabet simplicity-based detection," *IEEE Access*, vol. 8, pp. 21742–21758, 2020.

[42] H.-T. Wai, W.-K. Ma, and A. M. So, "Cheap semidefinite relaxation MIMO detection using row-by-row block coordinate descent," in *Proc. IEEE Int. Conf. Acoust., Speech Signal Process. (ICASSP)*, May 2011, pp. 3256–3259.

[43] M. A. Albreem, M. Juntti, and S. Shahabuddin, "Massive MIMO detection techniques: A survey," *IEEE Commun. Surveys Tuts.*, vol. 21, no. 4, pp. 3109–3132, 4th Quart., 2019.

[44] J. Wang, S. Kwon, and B. Shim, "Generalized orthogonal matching pursuit," *IEEE Trans. Signal Process.*, vol. 60, no. 12, pp. 6202–6216, Dec. 2012.

[45] A. Kurniawan, A. R. Danisya, and A. F. Isnawati, "Performance of mmWave channel model on 28 GHz frequency based on temperature effect in Wonosobo city," in *Proc. IEEE Int. Conf. Commun., Netw. Satell. (Comnetsat)*, Dec. 2020, pp. 37–41.

[46] S. Axler, *Linear Algebra Done Right*. Cham, Switzerland: Springer, 1997.

BAGHDAD HADJI received the State Engineering degree from the University of Tlemcen, Algeria, in 2010, and the M.S. degree in signal processing from the Military Polytechnic School, Algiers, Algeria, in 2016. He is currently pursuing the Ph.D. degree in telecommunication with the University of Science and Technology Houari Boumediene (USTHB), Algiers. His current research interests include signal processing techniques for future wireless communication, such as hybrid precoding and combining for mmWave MIMO transceivers, mmWave MIMO channel estimation with low complexity, and compressed sensing theory and its applications.

ABDELDJALIL AÏSSA-EL-BEY (Senior Member, IEEE) received the State Engineering degree from Ecole Nationale Polytechnique (ENP), Algiers, Algeria, in 2003, the M.S. degree in signal processing from Supelec and Paris XI University, Orsay, France, in 2004, and the Ph.D. degree in signal and image processing from ENST Paris, France, in 2007. In 2007, he joined the Signal and Communications Department, IMT Atlantique (Telecom Bretagne), Brest, France, as an Associate Professor, where he has been a Professor, since 2015. He was a Visiting Researcher with the Fujitsu Laboratories, Japan, in 2010, and the Department of Electrical and Electronic Engineering, The University of Melbourne, Australia, in 2015. His current research interests include blind source separation, blind system identification and equalization, compressed sensing, sparse signal processing, statistical signal processing, wireless communications, and adaptive filtering.

LAMYA FERGANI received the Ph.D. degree in electronics and signal processing from the University of Science and Technology Houari Boumediene, Algiers. She is currently a Professor and the Research Director of the University of Science and Technology Houari Boumediene. She has several research records and supervised Ph.D. candidates. Her current research interests include cognitive radio, wireless communications, signal processing, USRP, data analytics, and RFID signal processing.

MUSTAPHA DJEDDOU received the State Engineering degree from Ecole Militaire Polytechnique (EMP), Algiers, Algeria, and the M.S. and Ph.D. (Hons.) degrees in electrical engineering from the National Polytechnic School (ENP), Algiers, in 1998 and 2005, respectively. He was a Visiting Researcher with the Signal Processing Group, Darmastadt University, Germany, in 2003, and the Department of Computer Science and Statistics, Universidad sssRey Juan Carlos, Madrid, Spain, in 2008. From 2008 to 2017, he headed the Telecommunications Laboratory, Ecole Militaire Polytechnique. Currently, he is a Senior Lecturer with the National Polytechnic School, Algiers. His current research interests include statistical signal processing, applied signal processing for digital communication, and wireless communication.